Interpreting the dynamic pathogenesis of Parkinson's disease by longitudinal blood transcriptome analysis

Gang Xue[1,4], Gang Wang[1,2,4], Qianqian Shi[1], Hui Wang[1], Bo-Min Lv[1], Min Gao[1,3], Xiaohui Niu[1*] and Hong-Yu Zhang[1*]

[1]Hubei Key Laboratory of Agricultural Bioinformatics, College of Informatics, Huazhong Agricultural University, Wuhan, 430070, China

[2]Department of Basic Medical Laboratory, General Hospital of the Central Command Theater of PLA, Wuhan, 430015, China

[3]Lab of Epigenetics and Advanced Health Technology, Space Science and Technology Institute (Shenzhen), Shenzhen, 518117, China

[4]These authors contributed equally

*Corresponding authors: Hong-Yu Zhang (zhy630@mail.hzau.edu.cn) and Xiaohui Niu (niuxiaoh@mail.hzau.edu.cn)

Abstract

Achieving an improved understanding of the temporal sequence of factors involved in Parkinson's disease (PD) pathogenesis may accelerate drug discovery. In this study, we performed a longitudinal transcriptome analysis to identify associated genes underlying the pathogenesis of PD at three temporal phases. We firstly found that multiple initiator genes, which are related to processes of olfactory transduction and stem cell pluripotency, indicate PD risk to those subjects at the prodromal phase. And many facilitator genes involved in calcium signaling and stem cell pluripotency contribute to PD onset. We next identified 325 aggravator genes whose expression could lead to disease progression through damage to dopaminergic synapses and ferroptosis via an integrative analysis with DNA methylation. Last, we made a systematic comparison of gene expression patterns across PD development and accordingly provided candidate drugs at different phases in an attempt to prevent the neurodegeneration process.

Introduction

Parkinson's disease (PD) is a common chronic neurodegenerative disorder characterized by tremor and postural instability in motor symptoms along with non-motor symptoms, including hyposmia, sleeping disorder and cognitive decline[1,2]. The primary pathological features of PD are aggregations of alpha-synuclein (α-syn) in the cytoplasm, as well as the elimination of dopaminergic neurons in the substantia nigra pars compacta (SNc)[1].

Currently, the pathogenesis of PD has not been thoroughly elucidated, and many factors have been identified to contribute to the neurodegenerative process of PD. Recently, a new conceptual model of PD pathogenesis was proposed, in which these multifaceted factors can be divided into three temporal phases, namely, triggers, facilitators, and aggravators, and they may play distinct roles at different phases of PD[3]. Triggers are agents, such as environmental toxins and viral infections, that initiate the disease process. Accompanying or following triggers, facilitators spread the pathology to the central nervous system, leading to the onset of PD motor symptoms. Facilitators are proposed to include systemic inflammation, mitochondrial dysfunction, and genetic mutations. After PD manifests, aggravators, such as impaired autophagy and neuroinflammation, can directly contribute to disease progression. This conceptual model provides a new definition for PD pathogenesis, but the framework requires further investigation and validation at the molecular level. Elucidating the temporal sequence of pathogenesis in the disease process may be helpful for applying appropriate therapeutic agents when the related factor is most active[3].

53 Transcriptome sequencing is a useful technique that is employed to quantitatively
54 investigate genes responsible for the underlying pathogenesis. Previous transcriptomic
55 studies of PD examined gene expression at a single time point[4,5,6], hindering the
56 observation of expression changes in disease development. By monitoring the same
57 individual at different stages or time points, longitudinal transcriptomics analysis can
58 capture the gene expression patterns during the temporal phases of disease
59 and therefore has the potential to be employed to study the systemic evolution of
60 pathogenesis[7]. The Parkinson's Progression Markers Initiative (PPMI) is a landmark
61 longitudinal observational study to comprehensively evaluate PD and identify
62 biomarkers of disease progression[8]. In 2019, the PPMI reported the longitudinal RNA
63 resource of whole blood samples, which enabled us to determine the sequence of
64 pathogenesis in PD development.

65 In this study, we performed a longitudinal transcriptome analysis with blood samples
66 from the PPMI to study the dynamic pathogenesis of PD (Fig. 1). By analyzing the
67 subjects who developed from prodromal to PD, we first identified initiator genes that
68 indicated the risk of disease by survival analysis. Next, facilitator genes were
69 determined to contribute to the onset of PD through differential expression analysis.
70 Moreover, aggravator genes were identified in 252 *de novo* PD patients observed from
71 baseline to the third year. Causal inference and methylome-wide association study
72 (MWAS) provided further validation and insight into aggravation. Based on the distinct
73 gene expression patterns observed in these three phases, we suggested potential
74 therapies to be employed at the appropriate stages to prevent neurodegeneration in PD.

Notably, we demonstrated that withaferin A has the ability to promote the differentiation of neural stem cells into dopaminergic neurons *in vitro* experiment. The results suggest great potential of withaferin A to treat prodromal or early stage PD patients.

Results

Overview of study

In this study, two cohorts from PPMI were utilized to interpret the dynamic pathogenesis of PD (Fig. 1). Sixty-four prodromal subjects who had a diagnosis of hyposmia or rapid eye movement sleep behavior disorder (RBD) or at least one motor symptom of PD were followed from 2013 to 2019, some of whom had converted to PD during longitudinal observation. The conversion process was employed to infer the pathogenesis of initiation and facilitation. To investigate the pathogenesis of disease aggravation, 252 *de novo*, untreated idiopathic PD patients were selected at baseline and subsequently observed at 1 year, 2 years, and 3 years. In this instance, the Movement Disorder Society-Unified Parkinson's Disease Rating Scale (MDS-UPDRS) total score was applied to measure the clinical severity of PD.

It is difficult to obtain brain transcriptomes from PD patients, while blood transcriptomes are more accessible and less invasive to obtain from patients, making it easy to dynamically monitor cellular injuries that occur in PD. RNA-seq data were obtained from whole blood samples under the stringent quality controls applied by PPMI (Methods). Notably, ~60-70% of genes expressed in the blood are also expressed in brain tissues, as determined by examining mRNA only, suggesting that the blood

may serve as a surrogate tissue for brain transcriptome analysis and facilitate the identification of PD-related molecular signatures.

Identification of initiators

In the previous conceptual model of PD pathogenesis, triggers are agents or events that initiate disease pathogenesis during prodromal PD. These triggers, such as pathogens and environmental toxins, are exogenous factors that initiate the disease process[3]. However, we attempted to infer endogenous factors at the molecular level by examining initiator genes, which might indicate the risk of disease and are thought to act in the prodromal stage. To identify these genes, we defined prodromal conversion to PD as an "event" and defined time interval of conversion as the "survival time" to perform survival analysis (Methods). Next, genes that were significantly associated with the risk of conversion were considered initiator genes of PD (2,714 genes, log-rank test $P \leq 0.05$, Supplementary Table 1).

Many initiator genes that influence the risk of PD onset were involved in signaling pathways regulating pluripotency of stem cells, olfactory transduction, and hepatitis C (Fig. 2a). In line with the triggers proposed, hepatitis C, which is an infectious pathogen, is associated with a higher risk of developing PD[9]. In addition, the dysfunction of olfactory transduction is strongly related to hyposmia, which is one of the earliest non-motor symptoms of PD[10] and is consistent with the clinical symptoms of prodromal subjects, as previously described. Together with the evidence of α-syn aggregates in olfactory[11], these findings indicated that the olfactory system may be the major initiator

site in PD pathogenesis. Notably, *OR8D1*, one of the key genes to help maintain normal olfactory function[12], ranks first among the initiator genes (log-rank test, $P = 3.2e-05$). Prodromal subjects with lower expression levels of *OR8D1* were at high risk of converting to PD (Fig. 2b). Thus, the expression of *OR8D1* could be employed to help early diagnosis. In PD, ~50% of nigral neurons are lost before the onset of clinical motor symptoms[13]. According to our results, we hypothesize that the lost neurons might not be renewed due to the damaged pluripotency of stem cells, which can influence the neurogenesis process[14,15].

Identification of facilitators

Facilitators are proposed to help initiators spread PD pathology and damage the central nervous system[3]. Unlike initiator genes, facilitator genes are thought to contribute to the onset of PD and show different expression patterns in prodromal and early-stage PD. To find the facilitator genes, we identified differentially expressed genes (DEGs) by comparing the expression profiles from prodromal to confirmed PD patients in a discovery dataset, which contained 17 RNA-seq samples of five subjects during their natural conversion (Method, Fig. 3a). We identified 1,326 DEGs whose changes in expression during conversion may facilitate the onset of PD ($P \leq 0.05$, Supplementary Table 2). To assess the robustness of our results, a similar analysis was performed in a validation dataset with 57 prodromal subjects and 390 PD subjects at baseline. Although these two cohorts have no conversion relationship between each other, the large-scale samples can largely eliminate the influence of differences deriving from

genetic background in our comparative research. The DEGs in the discovery and validation datasets (false discovery rate (FDR) ≤ 0.01, Supplementary Table 3) had a significant overlap (Fig. 3b), supporting the results in the discovery dataset with limited samples. Therefore, these 1,326 DEGs refer to facilitator genes of PD.

The facilitator genes were mostly expressed in the cerebral cortex, suggesting that the central nervous system might have been damaged (Fig. 3c). In addition, the facilitator genes were mainly downregulated in the calcium signaling pathway and signaling pathways regulating pluripotency of stem cells during conversion (Fig. 3d). Evidence has shown that changes in calcium (Ca^{2+}) levels may trigger a series of events to increase SNc neuronal death sensitivity[16], including mitochondrial dysfunction, enhanced ROS generation and damaged ATP production. Ca^{2+} homeostasis is also regulated by PD-related proteins, such as α-syn, PINK-1/parkin, leucine-rich repeat kinase 2 (LRRK2), and DJ-1 protein[16]. These findings confirmed the facilitators of a previously conceptual model[3] and indicated that dysfunction in Ca^{2+} signaling is one of the earliest events in the pathogenesis of PD[16]. We also noted that the pathway of stem cells pluripotency was also captured by initiator genes; thus, the neurogenesis process was influenced in both the prodromal and early stages of PD, which may also imply its causative role in the onset of PD. Taken together, these findings indicated that the dysfunctions in calcium signaling and stem cell pluripotency might be considered facilitators of PD pathogenesis.

Identification of aggravators

163 Once PD manifests, aggravators can directly promote the neurodegenerative process
164 and contribute to disease progression. In fact, although there are some interventions for
165 PD, at present, there is no agent that can halt PD progression. Most of the patients
166 showed aggravation within a few years after diagnosis[17]. In addition, consistent with
167 our observation (Supplementary Fig. 1a-b), the clinical manifestations of patients differ
168 greatly in the trajectory of aggravation[18], hindering efforts to identify a suitable
169 treatment. Although molecular mechanism underlying PD aggravation has critical
170 importance in the long-term prevention and treatment of this disease, it has not been
171 elucidated to date. Therefore, we searched for potential aggravator genes to determine
172 the underlying mechanisms of PD.

173 With the longitudinal blood transcriptome of 252 patients at four serial time points
174 (baseline, 1 year, 2 years, and 3 years), we constructed linear mixed effects models
175 (Methods) to characterize the association between gene expression change and clinical
176 severity during disease aggravation. Using each subject's baseline samples as their own
177 control, this analysis reduces the noise derived from the genetic background of patients
178 and improves the precision. We identified 325 genes significantly associated with PD
179 aggravation (FDR $\leq$ 0.05; Supplementary Table 4), 307 of which were consistently
180 downregulated and 18 of which were upregulated, across the entire aggravation process
181 (Fig. 4a). Taking downregulated aggravator genes as an example, at early stages
182 (baseline and 1 year), these genes were expressed at a relatively high level, but the gene
183 expression level decreased significantly in many patients after 2-3 years. Such an
184 expression trend was also observed in an independent dataset from PD patients

185 (Supplementary Fig. 2), suggesting that the dynamic molecular functions dominating
186 disease aggravation may help the development of drugs to intervene in the process.
187 Moreover, the downregulated aggravator genes were mainly enriched in the
188 dopaminergic synapse pathway, cGMP-PKG signaling pathway, and ferroptosis (Fig.
189 4b). It is clear that the suppressed function of dopaminergic synapses can damage
190 dopaminergic neurons. Ferroptosis is an iron-dependent autophagic cell death process[19],
191 and prior research has elucidated its mechanism in PD neurodegeneration. For example,
192 as a key component of ferroptosis, iron generates hydroxyl radicals and induces the
193 oxidation of dopamine, which may lead to an oxidative environment and thus contribute
194 to the death of dopaminergic neurons in the SNc[20].

195 What remained to be confirmed was whether the changes in the expression levels of
196 aggravator genes were the consequences or causes of PD progression. Therefore, we
197 next performed cross-lagged panel analyses (Methods, Fig. 4c) to investigate the cause-
198 effect relationship between the 325 aggravator genes and clinical severity (i.e., MDS-
199 UPDRS total score). Ten aggravator genes showed significant path coefficients (β_4)
200 from baseline gene expression to follow-up MDS-UPDRS total score (the third year)
201 but did not show significant path coefficients (β_2) from baseline MDS-UPDRS total
202 score to follow-up gene expression, demonstrating that the changes in expression
203 exhibited by these genes may be the causes, rather than the consequences of PD
204 aggravation (Supplementary Table 5). Based on the unidirectional relationship from
205 baseline gene expression to follow-up clinical severity at ten genes, we further
206 examined the association between weighted gene expression risk score (ERS) at

207 baseline and MDS-UPDRS total score at follow-up and found a significant positive
208 correlation between them (Methods), which confirmed that these genes drive the
209 process of aggravation and could be utilized for disease prediction (Fig. 4d).
210

211 **Integrative analysis of aggravator genes and DNA methylation**

212 As is well-known, the alterations of gene expression are affected by comprehensive
213 factors, such as genetic variation and epigenetic changes. In this study, we further
214 integrated the baseline blood methylation profiles to elucidate the epigenetic regulation
215 related to disease aggravation. Methylome-wide association study (MWAS) were
216 performed to distinguish the disease signals from CpG methylation (Method). Since
217 methylation alterations may achieve long-term regulation of disease development and
218 do not cause clinical manifestations immediately[21,22] (Supplementary Fig. 3), we
219 constructed a linear model with the baseline methylome and the rate of PD aggravation.
220 A total of 1,416 CpG sites ($P \leq 0.001$, Supplementary Table 6) were found to be
221 associated with the rate of aggravation (Fig. 5a), and methylation score derived from
222 these CpG sites accounted for approximately 19% of its variance (Method, Fig. 5b). In
223 addition, previous research identified 138 CpGs that significantly changed over time in
224 PD patients with longitudinal genome-wide methylation data[23]. Although there is no
225 overlap between our aggravator rate-associated CpGs and the previously identified 138
226 CpGs, the genes mapped by CpGs showed significant overlap (P = 7.8e-06, Fig. 5c),
227 further indicating that these 1,416 CpGs identified by us were related to disease
228 aggravation. Moreover, the aberrant methylation events that occurred in many PD-

229 related pathways overlapped with those pathways enriched by aggravator genes, e.g.,
230 dopaminergic synapse and ferroptosis, which led us to investigate their functional
231 associations.

232 We subsequently explored the associations between our aggravator genes and these
233 aggravator rate-associated CpGs (Method) and found that the changes in expression in
234 all aggravator genes exhibited significant relationships with these CpGs ($P \leq 0.05$). In
235 particular, cg13298827 was positively correlated with expression changes of *PCDHA11*
236 located within +/-10 kb (Fig. 5d). *PCDHA11* may be involved in the creation and
237 maintenance of specific neuronal connections in the brain, and its dysfunction may
238 influence the signaling and communication between neural cells, thereby leading to the
239 aggravation of PD. Since some regulations may have long-range interactions, we next
240 integrated high-throughput chromosome conformation capture (Hi-C) data from the
241 brain dorsolateral prefrontal cortex[24] (http://resource.psychencode.org) and identified
242 18 CpG-gene interactions in the topologically associating domains (TADs)
243 (Supplementary Table 7). For example, cg17512517 may influence disease aggravation
244 by negatively regulating expression changes of *CCDC50* (Fig. 5d). Taken together, our
245 results indicated that DNA methylation may regulate the changes in expression levels
246 of aggravator genes, which may modulate PD progression.

247

248 **Inferred cellular changes associated with aggravation**

249 In addition to identifying genes associated with aggravation, we also examined which
250 cell types were changed along with PD aggravation. In this study, we applied the xCell

algorithm[25] to infer the abundance scores of 64 immune and stromal cell types from the RNA-seq expression profiles of each PD sample at baseline and after 1-3 years. Analogous to our aggravator gene identification flow, 14 cell types were found to be significantly associated with PD aggravation (FDR $\leq$ 0.05, Supplementary Fig. 4). Remarkably, neurons, although slightly increased in the third year, significantly decreased overall with disease aggravation, which is in keeping with the loss of neurons observed in the SNc of PD patients[1]. In addition, some of the gene signatures of neurons were also downregulated aggravator genes, such as *NDRG4*, *PKIA*, *SHISA6*, *STX16*, *ZNF14*, and *ZNF606*, which confirmed our previous results. Nonetheless, it has not been determined whether changes in cellular proportions take place before transcriptomic changes or after them. Moreover, a recent study provided more detailed evidence regarding the cell types underlying the pathogenesis of PD based on single-cell transcriptomic data, demonstrating that cholinergic neurons, monoaminergic neurons, enteric neurons, and oligodendrocytes were related to PD and that these cells changed at the earliest stages of disease progression[26].

Distinct expression patterns between initiator, facilitator and aggravator genes

We next investigated how PD develops by tracking the trajectory of gene expression patterns. We first observed that the initiator, facilitator and aggravator genes have little overlap (Fig. 6a), which is reminiscent of the distinct biological processes of these three temporal phases, as previously discussed. When further investigating their connection in the protein-protein interaction (PPI) network, we observed that the facilitator genes

273 possess more degrees than initiator genes and tend to be located in the hub of the
274 network (Fig. 6b-c), while aggravator genes are located in the hub compared to the
275 facilitator genes (Fig. 6d-e). Since the expression changes in initiator genes precede the
276 facilitator genes and the changes in facilitator genes precede the aggravator genes, it
277 appears that the dysfunction first occurred in the signature genes at the early phase,
278 which would further spread the disease disturbance to spur neurodegeneration by giving
279 way to new signature genes, exhibiting dynamic pathogenesis in disease development
280 and implying that although distinct biological functions are presented by the three
281 temporal phase genes, they can connect to one another in various ways. This complex
282 evolution of pathogenesis may account for the difficulties in halting or slowing PD
283 development. Taken together, these results confirmed the difference in pathogenesis
284 among the three temporal phases of PD while also demonstrating the connections
285 among them.
286

287 **Identification of potential drugs for different phases of PD**

288 After elucidating the factors involved in PD pathogenesis in three temporal phases, we
289 next sought to identify potential therapies to reverse or slow the development of PD.
290 Currently, pharmacological treatment and deep brain stimulation are the main therapies
291 to alleviate the symptoms of PD, but they are unable to prevent the neurodegenerative
292 process[27,28]. Another promising therapy is cell-based treatments, which can replace lost
293 neurons with new and healthy neurons to reconstruct disrupted circuits[29,30,31]. We
294 propose that these therapies should be applied at the appropriate phase of PD to

295 maximize the chances of modifying the neurodegeneration process.

296 As mentioned above, the stem cell pluripotency was influenced in both the prodromal
297 and early stages of PD, and analysis of facilitator genes indicated that the signaling
298 pathways regulating the pluripotency of stem cells (KEGG ID: hsa04550) were
299 downregulated when prodromal subjects were converted to PD patients (Fig. 7a). This
300 result motivated us to seek novel candidate agonists to treat prodromal or early stage
301 PD patients by recovering the function of stem cells and promoting their
302 revitalization of neurons. To this end, L1000CDS[2] analysis was performed to identify
303 potential agents by upregulating the expression of DEGs in the hsa04550 pathway
304 (Methods, Supplementary Fig. 5a). Next, we obtained three candidate compounds, i.e.,
305 atorvastatin, curcumin and withaferin A (WFA), the former two of which have been
306 reported to promote the differentiation of neurons in neural stem cells (NSCs)[32,33].
307 Moreover, similar results were also obtained in the validation dataset using the same
308 approach (Supplementary Fig. 5a), indicating that WFA is of high confidence for
309 promoting NSCs differentiation into neurons.

310 To verify our inferences, we first evaluated the effects of WFA on the proliferation
311 and differentiation of NSCs *in vitro* (Methods). The optimum concentration for NSCs
312 differentiation was identified by the CCK8 test (Fig. 7b). Since NSCs will start to
313 differentiate spontaneously in the absence of basic fibroblast growth factor (bFGF)[34],
314 we applied WFA or DMSO (control) to treat NSCs without bFGF, and we assessed
315 differentiation by immunofluorescence staining. We observed that WFA can promote
316 NSCs to differentiate more neurons (Tuj^+ cells), fewer astrocytes ($GFAP^+$ cells) and

317 oligodendrocytes (GalC^{+} cells) compared with the DMSO-treated control group (Fig.
318 7c-d), which demonstrated that WFA can promote NSCs to differentiate into neurons.
319 Given that the loss of dopaminergic neurons is an important pathological change in
320 PD[1], we performed further experiments and observed that the proportion of
321 dopaminergic neurons (TH^{+} Tuj^{+} cells) in neurons (Tuj^{+} cells) under WFA treatment
322 was significantly higher than that in the control (Fig. 7e-f), suggesting that WFA can
323 effectively promote NSCs to differentiate into dopaminergic neurons. Moreover, five
324 WFA-regulated genes were identified from the DEGs (Supplementary Fig. 5a) and
325 further validated by quantitative RT-PCR (Supplementary Table 8, Fig. 7g).
326 Specifically, *FGF2*, *ID1*, and *TCF3* were upregulated, which is consistent with our
327 hypothesis that NSCs differentiation is promoted by upregulating the DEGs. While
328 *WNT6* and *WNT11* were downregulated, we speculated that the difference between
329 blood tissue and NSCs may lead to this inconsistency. Notably, *TCF3* is a
330 transcriptional regulator involved in the maintenance of neural stem cells[35]; thus, its
331 functional recovery probably promotes the revitalization of neurons. *TCF3* is also a hub
332 node in the network of initiator-facilitator genes (Fig. 6c). Taken together, these results
333 strongly indicated that WFA has considerable potential to cure prodromal and early-
334 stage PD by promoting the differentiation of NSCs into dopaminergic neurons.
335 With the aggravation of PD, we found that biological terms, such as dopaminergic
336 synapse and the cGMP-PKG signaling pathway, were also enriched by the drug targets
337 of PD, implying their connections in a biological context. Among our aggravator genes,
338 six downregulated aggravator genes were also drug targets of PD, and three of them

have agonists in the DrugBank database, which might be considered viable drugs in attempts to slow PD aggravation (Table 1). For example, by upregulating *DRD3* in the dopaminergic synapse pathway, levodopa may be suitable to treat patients with relatively more severe symptoms. In fact, levodopa is effective in controlling most motor symptoms and remains the gold standard in the drug treatment of PD[36]. Moreover, to yield more effective disease-modifying treatments, some of these agonists should be combined to target the various pathogeneses in aggravation. In addition, although *SLC18A1* is not a target of PD to date, it is located in the dopaminergic synapse pathway and connected to known drug targets by dopamine transduction. The downregulation of *SLC18A1* expression may lead to dysfunction of the synaptic vesicle circle, thereby accelerating the severity of the disease (Supplementary Fig. 5b); therefore it may be reasonable to consider *SLC18A1* as a potential target for the design of therapeutic interventions in the future.

Discussion

In this study, we identified distinct molecular patterns in the development of PD with a longitudinal blood transcriptomic analysis and provided a modified conceptual model for PD pathogenesis. The results of this study helped us to identify appropriate therapies for PD patients at different stages of the disease.

At the prodromal stage of PD, we found that olfactory-associated genes were first reflected in the initiation of the disease and subsequently provided a simple and effective method to help early diagnosis by examining the expression of the olfactory

361 receptor *OR8D1* in blood samples. Since hyposmia is also a clinical feature of early-
362 stage patients[10], our results could be coupled with clinical observations. Nonetheless,
363 the validity of these results should be confirmed in larger prospective experiments. In
364 addition, the expression of the initiator genes also supported that hepatitis C is a trigger
365 to spark the disease[3,9].

366 After the prodromal subjects were diagnosed as PD patients, the expression of the
367 facilitator genes indicated that dysfunction of calcium regulation might contribute to
368 neuronal death, and the neurons were unable to be renewed due to the decreased
369 pluripotency of stem cells. Changes in calcium levels can induce a series of events,
370 including mitochondrial dysfunction, enhanced ROS generation, and damaged ATP
371 production[16]. Calcium is also regulated by PD-related proteins, such as α-syn and
372 LRRK2[16]. These findings confirmed the facilitators of the previously proposed
373 conceptual model[3].

374 With the progression of PD, the expression of the aggravator genes showed that the
375 dysfunction of dopaminergic synapses, cGMP-PKG signaling, and ferroptosis may
376 represent the main factors of the neurodegeneration process. Ferroptosis is an
377 autophagic cell death process that contributes to autophagy activation[19]. In line with the
378 role played by aggravators in a previous conceptual model, these findings highlight the
379 importance of autophagy in disease aggravation[3]. Other aggravators identified by this
380 study need to be confirmed through further experiments. In addition, we noted that
381 although the expression levels of aggravator genes are significantly changed with
382 progression, the magnitude of these expression level changes was not dramatic (|log2

383 (third year/baseline)| ≤ 1). One of the reasons for this finding may be that PD injury
384 occurs in brain tissue; thus, signal intensity may be reduced when it reaches the
385 bloodstream. The blood environment may also possess biological signals from the
386 internal environment or other organs, which may interfere with the extraction of disease
387 signals. In addition, PD is a chronic disease; therefore, gene expression does not change
388 dramatically, which also highlights the necessity of conducting longitudinal studies that
389 can capture this moderate dynamic change. Interestingly, by integrating DNA
390 methylation, we observed that methylation alterations at baseline did not cause clinical
391 manifestations immediately but may have influenced the PD aggravation rate by
392 regulating the changes in expression levels of aggravator genes. A similar phenomenon
393 was also reported by other chronic conditions[21], making it possible to detect and
394 monitor PD aggravation earlier. However, it has not been determined how these CpGs
395 regulate gene expression changes and how long they are sustained.

396 According to the pathogenesis involved at different stages of PD, we further inferred
397 and demonstrated that WFA has the ability to promote the differentiation of neural stem
398 cells into dopaminergic neurons with strong potential to treat prodromal or early stage
399 PD patients (Fig. 7b-g). WFA is a major active component of *Withania somnifera*,
400 which has been demonstrated to protect dopaminergic neurons in Parkinsonian mouse
401 models and has exhibited a strong antioxidative effect[37]. Moreover, *Withania somnifera*
402 was also reported to treat other disorders related to the central nervous system[37]; thus,
403 the future research should investigate whether WFA has a similar mode of action in the
404 treatment of other diseases, such as Alzheimer's disease. For advanced PD patients, we

proposed a list of drugs, such as levodopa, droxidopa, and dextromethorphan, that may be employed to slow PD aggravation. The appropriate drug combination addressing multiple targets and pathogenesis would benefit severe patients. Moreover, our results may also lead to the reconsideration of previously failed clinical trials, which may have been performed in nonspecific PD patients[3].

Methods

Clinical data analysis of PD patients

In this study, the Movement Disorder Society-Unified Parkinson's Disease Rating Scale (MDS-UPDRS) total score, which relates to various aspects, including non-motor and motor symptoms, as well as motor complications[38], was applied to measure the severity of PD patients. A higher score indicates an individual with a more serious condition. For the use of PD medications, there are seven medical treatments defined in PPMI, including unmedicated, levodopa, and levodopa plus dopamine agonist. In this study, we simply classified patients as unmedicated and medicated for subsequent analyses; for age characteristics, patients were classified into three groups adopted from PPMI: group 1 (< 56 years), group 2 (56-65 years), group 3 (> 65 years). Missing values of demographic and clinical information were imputed using the median value.

Omics data and quality control

For RNA-seq data of whole blood samples, quality control and quantification of gene or transcript expression were applied by PPMI. Briefly, FASTQ files were merged and

427 aligned to GRCh37 (hs37d5) by STAR (v2.4K)[39]. The read counts of genes or
428 transcripts were calculated by FeatureCounts[40] and abundance estimates (transcripts per
429 million, TPM) via salmon[41]. Samples with obvious quality control issues, such as
430 gender mismatch, principal component analysis (PCA) outliers and low read counts,
431 were filtered. After quality control, most samples have a mean Spearman correlation (>
432 0.87) to all other samples. To reduce the influence of technical noise, we removed genes
433 with counts/TPM of 0 in more than 80% of the samples in the subsequent analysis.
434 Importantly, according to PPMI analysis, ~60-70% of genes in whole blood are also
435 expressed in brain tissue by examining mRNA expression only. Detailed information
436 regarding the RNA sequencing and quality control can be found on the PPMI website
437 (http://ppmi-info.org/).

438 For DNA methylation (DNAm) data of whole blood samples, PPMI applied the
439 Illumina Human Methylation EPIC array (alias 850K methylation array) to assess
440 methylation status over 850,000 methylation sites across the whole genome. The β
441 values for each probe, which ranged from 0 (no methylation) to 1 (100% methylation),
442 were utilized to measure the methylation level of the targeted CpG site. Quality control
443 included removing low-quality samples and probes, as well as normalizing blood cell
444 composition. On that basis, we also applied the following filtering criteria in this study[42]:
445 removal of probes targeting X and Y chromosomes (N = 19,701), removal of cross-
446 reactive probes on the EPIC array (N = 43,254), and removal of probes overlapping
447 genetic variants at targeted CpG sites (N = 12,510), leaving 792,150 CpG sites for the
448 subsequent analysis. CpGs mapped to genes according to GPL21145 from Gene

449 Expression Omnibus (GEO, http://www.ncbi.nlm.nih.gov/geo/).

450

451 **Identifying initiator genes**

452 Sixty-four prodromal subjects were recruited at baseline with a longitudinal
453 observation beginning in 2013, and 18 prodromal subjects converted to PD by 2019.
454 After matching RNA-seq samples and removing subjects without longitudinal
455 observation, 53 prodromal subjects were kept for the downstream analysis. To identify
456 initiator genes of PD, we defined prodromal conversion to PD as an "event" and
457 defined the time interval from prodromal to PD as the "survival time" to perform
458 survival analysis. For each gene, baseline prodromal subjects were divided into two
459 groups based on the median expression of the gene. Next, survival curves were
460 constructed by Kaplan-Meier survival curves, and the log-rank test was applied to
461 compare whether there was a significant difference in the overall conversion between
462 the two groups using the R package survival.

463

464 **Identifying facilitator genes**

465 To identify facilitator genes, we first performed differential expression analysis in a
466 discovery dataset, which contained 17 RNA-seq samples of five subjects after matching
467 clinical status and RNA-seq samples. Specifically, the heterogeneity between subjects
468 is an important confounding factor identified by PCA (Fig. 3a); thus, we applied
469 a multi-factor design that included the subjects and their condition (prodromal and PD)
470 information in the design formula to identify DEGs using the R package/Bioconductor

DESeq2[43]. This design will account for differences between the subjects when estimating the effect due to the condition. The validation dataset contained 57 prodromal and 390 PD RNA-seq samples at baseline without a conversion relationship between each other; therefore, the DEGs of the validation dataset were identified only by estimating the effect due to the condition.

Identifying aggravator genes

In this study, 252 PD patients both included clinical and RNA-seq data at four serial time points (baseline, 1-3 years). We first filtered the genes whose expression did not significantly change during the four time points based on repeated measures ANOVA with the R package ez. The *P*-value was adjusted by sphericity corrections followed by multiple testing using FDR. Genes with FDR $\leq$ 0.01 were kept for subsequent analyses (3435 genes). The linear mixed-effects model was constructed to identify which gene was associated with PD aggravation using the *lme* function in the R package nlme. Each model included the MDS-UPDRS total score as the dependent variable; gene expression, age, and time (i.e., baseline, 1-3 years), and medication (unmedicated or medicated) as fixed effects; Each subject variation was included as a random effect and considered their different response to medical treatment, therefore each model was constructed as follows:

MDS-UPDRS total score ~ Gene expression + Age + Time + Medication, random = ~1+ Medication | Subject.

Genes with FDR $\leq$ 0.05 were defined as aggravator genes (325 genes, Supplementary

Table 4). The β coefficient of the gene in the model lower than 0 indicates that it was downregulated with PD aggravation; otherwise, it was upregulated. The R package Pheatmap was subsequently used to plot the heatmap of aggravator genes. Notably, some PD samples were abandoned in the above analysis because they did not possess RNA-seq data for four serial years. In fact, most of them were measured three times, involving 425 RNA-seq samples, which were regarded as an independent dataset to assess the robustness of the aggravator genes.

Cross-lagged panel analysis

Cross-lagged panel analysis was used to investigate cause-effect relationship between the expression of aggravator genes and clinical severity (Fig. 4c). Briefly, baseline gene expression and MDS-UPDRS total score were adjusted for age by regression residual analyses and then standardized with Z-transformation (mean = 0, SD = 1). The same process was performed in the follow-up year (third year) with additional adjustment for the times of medical treatment. Then, two following equations were built:

$$X_{follow-up} = \beta_1 X_{baseline} + \beta_2 Y_{baseline} + \varepsilon_X$$

$$Y_{follow-up} = \beta_3 Y_{baseline} + \beta_4 X_{baseline} + \varepsilon_Y$$

Here, X is aggravator gene and Y is MDS-UPDRS total score. The linear regression coeffcients β_1 and β_3 describe the autoregressive effects, and the regression coeffcients β_2 and β_4 represent cross-lagged effects. All parameters and statistics were estimated by the *sem* function in the R package lavaan based on these two equations. Next, the weighted gene expression risk score (ERS) was calculated as follows:

$$\text{Weighted } ERS = \frac{1}{n}(\beta_1 \times Gene_1 + \beta_2 \times Gene_2 + \beta_3 \times Gene_3 + ... + \beta_{n\text{-}1} \times Gene_{n\text{-}1} + \beta_n \times Gene_n)$$

where β is the cross-lagged path coefficient (β_4) for each gene, and n is the number of genes included.

MWAS analysis

A linear regression model was constructed to assess the associations between each CpG's methylation level (β value) and clinical traits of PD at baseline (N = 330). The model used for each CpG was as follows:

MDS-UPDRS total score ~ Methylation β value + Age

Since variation of DNA methylation (DNAm) may arise prior to disease[21,22], and we hypothesized that DNAm may influence the aggravation of PD in a long-term manner, we applied the rate of PD aggravation, i.e., the change of MDS-UPDRS total score from baseline to third years, as clinical traits of PD to identify the aggravation rate-associated CpGs. After matching longitudinal clinical and DNAm data, 268 PD patients were retained for the subsequent analysis. Using the *lm* function in R, the linear regression model used for each CpG was as follows:

Rate of PD aggravation ~ Methylation β value + Age + Medication times

The quantile-quantile (Q-Q) plot was used to diagnose the above MWAS results using the R package qqman. To estimate how much of the rate of PD aggravation could be explained by blood DNAm, the top association CpGs were selected first ($P \leq 0.001$, Supplementary Table 6). Next, PCA was performed on these CpGs, and each patient was scored by the first principal component using the R package psych. A linear model

536 was constructed to measure the relationship between the score calculated by these CpGs
537 and the rate of PD aggravation.
538
539 **Functional analysis**
540 KEGG pathway enrichment and gene set enrichment analysis (GSEA) analysis (2000
541 total permutations) of gene sets were performed by the R/Bioconductor package
542 clusterProfiler[44]. Tissue enrichment analysis of DEGs between prodromal and PD was
543 investigated by R package/Bioconductor TissueEnrich[45].
544
545 **Integrating transcriptome and methylome on PD aggravation**
546 The RNA-seq profiles and DNA methylation array data were pairwise integrated (N =
547 191) to study the regulatory relationship between each aggravator gene and each
548 aggravation rate-associated CpG site. Each linear regression model included delta gene
549 expression level change from baseline to third years as the dependent variable (log2
550 (third year/baseline)), β value of a CpG site at baseline as the independent variable, and
551 age and medication times as covariates:
552 $$\Delta \text{ Gene expression level} \sim \text{Methylation } \beta \text{ value} + \text{Age} + \text{Medication times}$$
553
554 **xCell analysis**
555 xCell[25] was used to estimate the abundance scores of 64 immune and stromal cell types
556 from the RNA-seq profiles of each PD patent over time (i.e., baseline, 1, 2, 3 years),
557 the abundance scores was then standardized with Z-transformation (mean = 0, SD = 1)

558 Similar to our aggravator genes analysis, linear mixed-effects model was used to
559 inferred which cell type was associated with PD aggravation:

560 MDS-UPDRS total score ~ Cell score + Age + Medication, random = ~1+
561 Medication | Subject

562

563 **Observation of initiator, facilitator and aggravator genes in the PPI network**

564 The interactions between initiator, facilitator and aggravator genes were examined in a
565 protein-protein interaction (PPI) network. The PPI network was derived from the
566 STRING database (http://www.string-db.org), and the interaction with experimental
567 score higher than 400 was considered reliable. Notably, since it difficult to observe the
568 network relationship between aggravator genes and facilitator genes identified from the
569 discovery dataset, we merged the facilitator genes both from the discovery and
570 validation datasets to observe their connections with aggravator genes in the PPI
571 network. The gene networks were subsequently visualized using Cytoscape[46].

572

573 **Drug discovery by L1000CDS² analysis**

574 The Library of Integrated Network-based Cellular Signatures (LINCS) program has
575 generated more than 1 million transcriptional profiles to elaborate the human cell
576 expression change under different perturbations of agents[47]. The L1000 dataset is part
577 of LINCS, which is based on the expression of only ~1000 genes[48]. L1000CDS² is a
578 LINCS L1000 characteristic direction signature search engine that links drugs, genes,
579 and diseases by comparing the input signatures to the background

580 (http://amp.pharm.mssm.edu/L1000CDS2/#/index). In this study, we applied
581 L1000CDS² to predict potential small molecular compounds that may reverse the
582 expression of DEGs between prodromal and PD subjects.

583 In the discovery dataset, 50 agents were returned by L1000CDS² according to eight
584 DEGs ($P \leq 0.05$) in pathways of regulating pluripotency of stem cells (KEGG ID:
585 hsa04550). We further selected three candidate compounds, i.e., atorvastatin, curcumin
586 and withaferin A (WFA), which were used to treat patients with mental disorders in
587 clinical trials (https://clinicaltrials.gov/), indicating the ability of delivery across the
588 blood brain barrier. Using the same approach, WFA was also identified in the validation
589 dataset (57 prodromal and 390 PD RNA-seq samples). To identify potential genes
590 regulated by WFA, we further identified six DEGs in the discovery dataset that
591 overlapped with background genes of WFA in the L1000 dataset, and five of these six
592 potential WFA-regulated genes in the discovery dataset were confirmed by the
593 validation dataset (Supplementary Fig. 5a).

594

595 **Isolation and culture of rat fetal neural stem cells**

596 Rat fetal NSCs were isolated and cultured from brain tissues of Sprague-Dawley rats at
597 14−18 days post-coitum. Briefly, brain tissues were cut into small blocks, digested by
598 pre-warmed StemPro® Accutase (A11105-01, Gibco, NY, USA), filtered by a 70-μm
599 cell strainer (352350, BD Biosciences, NY, USA) and centrifuged. The cell pellet was
600 resuspended in pre-warmed StemPro® NSC SFM complete medium (consisting of
601 KnockOut D-MEM/F-12 with 2% StemPro® Neural Supplement, 20 ng/mL bFGF, 20

602 ng/mL EGF, and 1% GlutaMAX-I; A1050901, Gibco, NY, USA), inoculated in a dish
603 at 1×10^7/mL and incubated at 37°C, 5% CO_2 and 90% humidity. The NSCs that
604 developed into neurospheres were passaged after 5-7 days (Supplementary Fig. 6a). In
605 subculture, the NSCs were digested by pre-warmed StemPro® Accutase and plated in
606 dishes precoated with 20 μg/mL fibronectin (33016015, Gibco, NY, USA) to adherent
607 culture at 37°C, 5% CO_2 and 90% humidity (Supplementary Fig. 6b). The NSCs were
608 passaged again when 75-90% confluent. The cells were identified by
609 immunofluorescence staining of Nestin at passage 2 (P2) (Supplementary Fig. 6c-d).
610 All WFA effects research experiments were carried out on cells at passages 2 to 3 (P2~3)
611 to minimize the experimental deviations.
612
613 **Analysis of WFA on NSCs proliferation by CCK8 assay**
614 WFA (HY-N2065, MCE, NJ, USA) was dissolved in DMSO to make a 1 mmol/L stock
615 solution, and subsequently, we made culture media containing different concentrations
616 of WFA with StemPro® NSC SFM complete medium. The working concentrations of
617 WFA were 0, 2, 10, 50, 250, 1000, 5000, and 25000 nmol/L. After that step, rat fetal
618 NSCs at P2 were collected and resuspended in culture media containing WFA at
619 5×10^4/mL and then seeded at 100 μL/well in 96-well plates immediately. To minimize
620 the experimental deviations, culture medium containing WFA but without NSCs was
621 used as a blank control for each concentration. After incubating the cells at 37°C, 5%
622 CO_2 and 90% humidity for 48 hours, 10 μL CCK8 reagent (HY-K0301, MCE, NJ, USA)
623 was added to each well and incubated for 4 hours. The absorbance was measured at 450

624 nm using a microplate reader (Multiskan MK3, Thermo Fisher Scientific, MA, USA).
625 The working concentration of WFA with the highest average absorbance was used to
626 analyze the effect of WFA on NSCs differentiation.
627
628 **Intervention of NSCs differentiation by WFA**
629 Rat fetal NSCs at P3 were plated as an adherent culture on chamber slides (177380,
630 Thermo Fisher Scientific, MA, USA) or 6-well plates pre-coated with 20 μg/mL
631 fibronectin for 1 hour. To investigate the effect of WFA on NSCs differentiation, we
632 withdrew bFGF from StemPro® NSC SFM complete medium and added WFA stock
633 solution (1 mmol/L in DMSO, 1:4000; according to the experimental results of CCK8
634 assay, the work concentration is 250 nmol/L) or DMSO (D2438, 1:4000, Sigma, MO,
635 USA) into the media. Then, the cells were incubated at 37°C, 5% CO_2 and 90%
636 humidity until subsequent immunofluorescence and quantitative RT-PCR detection.
637
638 **Analysis of WFA on NSCs differentiation by immunofluorescence staining**
639 After intervention by WFA or DMSO for 48 hours, NSCs undergoing differentiation
640 were fixed, permeabilized and blocked and then incubated with primary mouse anti-
641 Tuj antibody (ab78078, 1:1000, Abcam, Cambridge, UK), primary mouse anti-GALC
642 antibody (MAB342, 1:100, Millipore, MA, USA) or primary rabbit anti-GFAP antibody
643 (16825-1-AP, 1:2000, ProteinTech, Wuhan, China) overnight at 4°C. After washing
644 with PBS, cells were incubated with Alexa Fluor 594 conjugated goat anti-mouse IgG
645 (H+L) cross-adsorbed secondary antibody (A-11005, 1:200, Thermo Fisher Scientific,

646 MA, USA) or Alexa Fluor 488 conjugated goat anti-rabbit IgG (H+L) cross-adsorbed
647 secondary antibody (A-11008, 1:200, Thermo Fisher Scientific, MA, USA) at 37°C for
648 30 min. Finally, cells were washed with PBS, dyed with DAPI (Roche, Basel,
649 Switzerland), mounted with 50% glycerol/PBS and photographed under a fluorescence
650 microscope (BX51, Olympus, Tokyo, Japan).

651 After treating NSCs with WFA or DMSO for seven days, double
652 immunofluorescence staining of Tuj and tyrosine hydroxylase (TH) was used to analyze
653 whether WFA could further affect NSCs differentiation into dopaminergic neurons.
654 Briefly, after fixation, permeabilization and blocking, cells were incubated with both
655 primary mouse anti-Tuj antibody and primary rabbit anti-TH antibody (ab112, 1:1000,
656 Abcam, Cambridge, UK) overnight at 4°C. Then, the cells were incubated with mixed
657 secondary antibodies of Alexa Fluor 594-conjugated goat anti-mouse IgG and Alexa
658 Fluor 488-conjugated goat anti-rabbit IgG for 30 min. Finally, the cells were dyed with
659 DAPI, mounted with 50% glycerol/PBS and photographed under a BX51 fluorescence
660 microscope.

661

662 **Quantitative RT-PCR**

663 Total RNA was extracted from NSCs treated with WFA or DMSO for 48 hours with
664 TRIzol reagent (15596026, Thermo Fisher Scientific, MA, USA) and reverse
665 transcribed into cDNA using the RevertAid RT Reverse Transcription Kit (K1691,
666 Thermo Fisher Scientific, MA, USA). Then, qRT-PCR mixtures were prepared with the
667 KAPA SYBR® FAST Universal qPCR Kit (KK4601, Sigma, MO, USA) according to

the manufacturer's instructions and run in LightCycler 96 (Roche, Switzerland). The mRNA expression of genes regulating the pluripotency of stem cells was normalized to the expression of GAPDH. The results were compared by the 2−ΔΔCt method. The specific primers (Supplementary Table 8) were synthesized by Tsingke Biological Technology (Wuhan, China).

Statistical analysis of NSCs experiments

Image-Pro Plus 6.0 software (Media Cybernetics, MA, USA) was used for analysis and cell counting of the fluorescence images. The results from different groups were compared using Student's *t*-test or one-way ANOVA followed by Tukey's multiple comparison tests. P-value $\leq$ 0.05 was considered to be significant. All statistical analyses were performed with GraphPad Prism 6 software (GraphPad Software, CA, USA).

PD drugs and targets collection

The drugs for PD were obtained from clinical trials (release 2019.4.22, at least phase 2 clinical trial drugs, https://clinicaltrials.gov/), and the drug targets were extracted from DrugBank[49], DGIdb[50] and TTD[51]. We finally collected 104 PD drugs corresponding to 363 target genes (Supplementary Table 9).

Data availability

Data used in this study were obtained from the Parkinson's Progression Markers

Initiative (PPMI) database (www.ppmiinfo.org/data). For up-to-date information on the study, please visit www.ppmiinfo.org.

Acknowledgments

We would like to acknowledge PPMI - a public-private partnership, which is funded by the Michael J. Fox Foundation for Parkinson's Research and funding partners, including Abbvie, Allergan, Amathus Therapeutics, Avid Radiopharmaceuticals, Biogen, BioLegend, Bristol-Myers Squibb, Calico, Celgene, Denali, GE Healthcare, Genetech, GlaxoSmithKline, Golub Capital, Handl Therapeutics, Insitro, Janssen Neuroscience, Lilly, Lundbeck, Merck, Meso Scale Discovery, Pfizer, Piramal, Prevail, Roche, Sanofi Genzyme, Servier, Takeda, Teva, UCB, Verily, and Voyager Therapeutics. We also thank the National Natural Science Foundation of China (grant 31670779) for supporting this study.

Author contributions

H.Y.Z. and X.H.N. conceived the project; G.X. collected and performed data analysis with help from X.H.N., Q.Q.S., M.G., and H.W; G.W. performed the WFA experiment. G.X., G.W., Q.Q.S., H.Y.Z., X.H.N., H.W., and B.L wrote and edited the manuscript.

Competing interests

The authors declare no competing interests.

711 **References**

712 1. Dauer W, Przedborski S. Parkinson's disease: mechanisms and models. *Neuron*
713 **39**, 889-909 (2003).
714 2. Chaudhuri KR, Healy DG, Schapira AH. Non-motor symptoms of Parkinson's
715 disease: diagnosis and management. *Lancet Neurol.* **5**, 235-245 (2006).
716 3. Johnson ME, Stecher B, Labrie V, Brundin L, Brundin P. Triggers, facilitators,
717 and aggravators: Redefining Parkinson's disease pathogenesis. *Trends Neurosci.*
718 **42**, 4-13 (2019).
719 4. Shamir R*, et al.* Analysis of blood-based gene expression in idiopathic
720 Parkinson disease. *Neurology* **89**, 1676-1683 (2017).
721 5. Chen-Plotkin AS. Blood transcriptomics for Parkinson disease? *Nat. Rev.*
722 *Neurol.* **14**, 5-6 (2018).
723 6. Fan Y, Xiao S. Progression rate associated peripheral blood biomarkers of
724 Parkinson's disease. *J. Mol. Neurosci.* **65**, 312-318 (2018).
725 7. Androulakis IP, Yang E, Almon RR. Analysis of time-series gene expression
726 data: methods, challenges, and opportunities. *Annu. Rev. Biomed. Eng.* **9**, 205-
727 228 (2007).
728 8. Marek K*, et al.* The parkinson progression marker initiative (PPMI). *Prog.*
729 *Neurobiol.* **95**, 629-635 (2011).
730 9. Kim J-M*, et al.* Association between hepatitis C virus infection and Parkinson's
731 disease. *Mov. Disord*. **31**, 1584-1585 (2016).
732 10. Doty RL. Olfaction in Parkinson's disease and related disorders. *Neurobiol. Dis.*

733 **46**, 527-552 (2012).

734 11. Braak H, Del Tredici K, Rüb U, De Vos RA, Steur ENJ, Braak E. Staging of
735 brain pathology related to sporadic Parkinson's disease. *Neurobiol. Aging.* **24**,
736 197-211 (2003).

737 12. Mainland JD*, et al.* The missense of smell: functional variability in the human
738 odorant receptor repertoire. *Nat. Neurosci.* **17**, 114 (2014).

739 13. Ross GW*, et al.* Parkinsonian signs and substantia nigra neuron density in
740 decendents elders without PD. *Ann. Neurol.* **56**, 532-539 (2004).

741 14. Wichterle H, Przedborski S. What can pluripotent stem cells teach us about
742 neurodegenerative diseases? *Nat. Neurosci.* **13**, 800-804 (2010).

743 15. Le Grand JN, Gonzalez-Cano L, Pavlou MA, Schwamborn JC. Neural stem
744 cells in Parkinson's disease: a role for neurogenesis defects in onset and
745 progression. *Cell. Mol. Life Sci.* **72**, 773-797 (2015).

746 16. Calì T, Ottolini D, Brini M. Calcium signaling in Parkinson's disease. *Cell*
747 *Tissue Res.* **357**, 439-454 (2014).

748 17. Poewe W, Mahlknecht P. The clinical progression of Parkinson's disease.
749 *Parkinsonism Relat. Disord.* **15**, S28-S32 (2009).

750 18. Chenplotkin A*, et al.* Finding useful biomarkers for Parkinson's disease. *Sci.*
751 *Transl. Med.* **10**, eaam6003 (2018).

752 19. Gao M, Monian P, Pan Q, Zhang W, Xiang J, Jiang X. Ferroptosis is an
753 autophagic cell death process. *Cell Res.* **26**, 1021-1032 (2016).

754 20. Guiney SJ, Adlard PA, Bush AI, Finkelstein DI, Ayton S. Ferroptosis and cell

755 death mechanisms in Parkinson's disease. *Neurochem. Int.* **104**, 34-48 (2017).

756 21. Chen R*, et al.* Longitudinal personal DNA methylome dynamics in a human
757 with a chronic condition. *Nat. Med.* **24**, 1930-1939 (2018).

758 22. Rakyan VK, Down TA, Balding DJ, Beck S. Epigenome-wide association
759 studies for common human diseases. *Nat. Rev. Genet.* **12**, 529-541 (2011).

760 23. Henderson-Smith A*, et al.* DNA methylation changes associated with
761 Parkinson's disease progression: outcomes from the first longitudinal genome-
762 wide methylation analysis in blood. *Epigenetics* **14**, 365-382 (2019).

763 24. Wang D*, et al.* Comprehensive functional genomic resource and integrative
764 model for the human brain. *Science* **362**, (2018).

765 25. Aran D, Hu Z, Butte AJ. xCell: digitally portraying the tissue cellular
766 heterogeneity landscape. *Genome Biol.* **18**, 220 (2017).

767 26. Bryois J*, et al.* Genetic identification of cell types underlying brain complex
768 traits yields insights into the etiology of Parkinson's disease. *Nat. Genet.* **52**,
769 482-493 (2020).

770 27. Connolly BS, Lang AE. Pharmacological treatment of Parkinson disease: a
771 review. *JAMA* **311**, 1670-1683 (2014).

772 28. Benabid AL, Chabardes S, Mitrofanis J, Pollak P. Deep brain stimulation of the
773 subthalamic nucleus for the treatment of Parkinson's disease. *Lancet Neurol.* **8**,
774 67-81 (2009).

775 29. Barker RA, Drouin-Ouellet J, Parmar M. Cell-based therapies for Parkinson
776 disease—past insights and future potential. *Nat. Rev. Neurol.* **11**, 492 (2015).

30. Reddy AP, Ravichandran J, Carkaci-Salli N. Neural regeneration therapies for Alzheimer's and Parkinson's disease-related disorders. *Biochim. Biophys. Acta Mol. Basis. Dis.* **1866**, 165506 (2020).

31. Qian H*, et al.* Reversing a model of Parkinson's disease with in situ converted nigral neurons. *Nature* **582**, 550-556 (2020).

32. Choi N-Y*, et al.* Atorvastatin rejuvenates neural stem cells injured by oxygen-glucose deprivation and induces neuronal differentiation through activating the PI3K/Akt and ERK pathways. *Mol. Neurobiol.* **56**, 2964-2977 (2019).

33. Chen F*, et al.* Curcumin increased the differentiation rate of neurons in neural stem cells via wnt signaling in vitro study. *J. Surg. Res.* **192**, 298-304 (2014).

34. Gage FH. Mammalian neural stem cells. *Science* **287**, 1433-1438 (2000).

35. Ohtsuka T*, et al.* Gene expression profiling of neural stem cells and identification of regulators of neural differentiation during cortical development. *Stem Cells* **29**, 1817-1828 (2011).

36. Poewe W, Antonini A, Zijlmans JC, Burkhard PR, Vingerhoets F. Levodopa in the treatment of Parkinson's disease: an old drug still going strong. *Clin. Interv. Aging* **5**, 229 (2010).

37. Singh N, Rai SN, Singh D, Singh SP. Withania somnifera shows ability to counter Parkinson's Disease: An Update. *SOJ Neurol.* **2**, 1-4 (2015).

38. Goetz CG*, et al.* Movement Disorder Society-sponsored revision of the Unified Parkinson's Disease Rating Scale (MDS-UPDRS): Scale presentation and clinimetric testing results. *Mov. Disord.* **23**, 2129-2170 (2008).

799 39. Dobin A, *et al.* STAR: ultrafast universal RNA-seq aligner. *Bioinformatics* **29**,
800 15-21 (2013).
801 40. Liao Y, Smyth GK, Shi W. featureCounts: an efficient general purpose program
802 for assigning sequence reads to genomic features. *Bioinformatics* **30**, 923-930
803 (2014).
804 41. Patro R, Duggal G, Love MI, Irizarry RA, Kingsford C. Salmon provides fast
805 and bias-aware quantification of transcript expression. *Nat. Methods.* **14**, 417-
806 419 (2017).
807 42. Pidsley R, *et al.* Critical evaluation of the Illumina MethylationEPIC BeadChip
808 microarray for whole-genome DNA methylation profiling. *Genome Biol.* **17**,
809 208 (2016).
810 43. Love MI, Huber W, Anders S. Moderated estimation of fold change and
811 dispersion for RNA-seq data with DESeq2. *Genome Biol.* **15**, 550 (2014).
812 44. Yu G, Wang L-G, Han Y, He Q-Y. clusterProfiler: an R package for comparing
813 biological themes among gene clusters. *OMICS.* **16**, 284-287 (2012).
814 45. Jain A, Tuteja G. TissueEnrich: Tissue-specific gene enrichment analysis.
815 *Bioinformatics* **35**, 1966-1967 (2019).
816 46. Shannon P, *et al.* Cytoscape: a software environment for integrated models of
817 biomolecular interaction networks. *Genome Res.* **13**, 2498-2504 (2003).
818 47. Keenan AB, *et al.* The library of integrated network-based cellular signatures
819 NIH program: system-level cataloging of human cells response to perturbations.
820 *Cell Syst.* **6**, 13-24 (2018).

821 48. Subramanian A*, et al.* A next generation connectivity map: L1000 platform and
822 the first 1,000,000 profiles. *Cell* **171**, 1437-1452. e1417 (2017).
823 49. Law V*, et al.* DrugBank 4.0: shedding new light on drug metabolism. *Nucleic*
824 *Acids. Res.* **42**, D1091-D1097 (2014).
825 50. Wagner AH*, et al.* DGIdb 2.0: mining clinically relevant drug–gene interactions.
826 *Nucleic Acids. Res.* **44**, D1036-D1044 (2016).
827 51. Qin C*, et al.* Therapeutic target database update 2014: a resource for targeted
828 therapeutics. *Nucleic Acids. Res.* **42**, D1118-D1123 (2014).

829 **Figure**

830

831 **Fig. 1 Study workflow.** Longitudinal RNA-seq of whole blood samples and
832 corresponding clinical assessment were obtained from Parkinson's Progression
833 Markers Initiative (PPMI) database (https://www.ppmi-info.org/data). (up) Flowchart
834 of analysis in the conversion process. (right) Flowchart of analysis in the aggravation
835 process.

836

837 **Fig. 2 Pathway enrichment and survival analysis of initiator genes. a** KEGG
838 pathway enrichment of initiator genes by gene set enrichment analysis (GSEA) (genes
839 ranked by -log10(*P*-value)). **b** Kaplan-Meier curves of conversion in prodromal
840 subjects ($N = 53$). The magenta line indicates prodromal subjects with higher expression
841 of *OR8D1*, while the blue line indicates prodromal subjects with lower expression of
842 *OR8D1*, which are at high risk of conversion.

843

844 **Fig. 3 Identifying DEGs between prodromal and PD. a** PCA clustering plot of RNA-
845 seq data between prodromal and PD. **b** Overlaps of DEGs in the discovery and
846 validation datasets ($P = 4.75e-09$). **c** Tissue enrichment of DEGs between prodromal
847 and PD (*$P \leq 0.05$). **d** KEGG pathway enrichment of DEGs by GSEA (genes ranked
848 by log2FoldChange).

849

850 **Fig. 4 Functional analysis of aggravator genes and causal inference. a** Heatmap of

851 aggravator genes in longitudinal PD patients (N = 252). **b** KEGG pathway enrichment
852 of downregulated aggravator genes. **c** Causal inference based on the cross-lagged path
853 analysis model. β_2 and β_4 are cross-lagged path coefficients. Genes with significant
854 unidirectional paths (β_4, $P \leq 0.05$) from baseline gene expression to follow-up MDS-
855 UPDRS total score (the third year), while those without significant path coefficients
856 (β_2) from baseline MDS-UPDRS total score to follow-up gene expression are
857 considered to be causing genes in disease aggravation. **d** Correlation between the
858 weighted gene expression risk score (ERS) at baseline and MDS-UPDRS total score at
859 follow-up (the third year).
860
861 **Fig. 5 Assessment of the blood methylome and investigation of their regulatory**
862 **relationship with aggravator genes. a** Quantile-quantile (Q-Q) plot of MWAS result
863 using rate of aggravation as clinical traits (N = 268). **b** Linear relationship between
864 DNA methylation score and rate of aggravation of PD patients. **c** Overlaps of our
865 aggravator rate associated-genes with literature-reported PD aggravator-associated
866 genes (CpGs map to genes). **d** (upside) The associations between cg13298827,
867 *PCDHA11* and aggravation; (downside) The associations between cg17512517,
868 *CCDC50* and aggravation. Positive (+) and negative (-) associations are shown in the
869 figure.
870
871 **Fig. 6 Relationship between initiator, facilitator and aggravator genes. a** Initiator,
872 facilitator and aggravator genes do not show significant overlaps with each other (P >

873 0.05). **b** Boxplot of the connected degrees of initiator and facilitator genes in the PPI
874 network. Facilitator genes showed more connections than initiator genes (P = 2e-04). **c**
875 Network diagram depicting the interaction between initiator and facilitator genes. The
876 facilitator genes (yellow) tend to be located in the hub of the network. **d** Boxplot of the
877 connected degrees of facilitator and aggravator genes in the PPI network. Aggravator
878 genes showed more connections than facilitator genes (P = 4.2e-09). **e** Network
879 diagram depicting the interaction between facilitator and aggravator genes. The
880 aggravator genes (pink) tend to be located in the hub of the network.
881
882 **Fig. 7 WFA promotes the proliferation and differentiation of NFCs. a** GSEA plot
883 showing downregulated signaling pathways regulating pluripotency of stem cells when
884 prodromal conversion to PD. **b** Identification of the optimum concentration of WFA on
885 the proliferation of NFCs by the CCK8 test. WFA significantly promoted NSCs
886 proliferation at 50, 250, and 1000 nmol/L (*$P \leq 0.05$), and the proliferative effects at
887 250 nmol/L were significantly higher than those at 50 nmol/L ($^{\#}P \leq 0.05$), suggesting
888 that WFA has a dose-dependent effect, whereas no significant difference was observed
889 between 250 nmol/L and 1000 nmol/L, indicating that 250 nmol/L may reach the
890 plateau stage of a dose-dependent effect; thus, 250 nmol/L was adopted to evaluate the
891 effects of WFA on the next NSCs differentiation experiment. **c** Detection of NFCs
892 differentiation by immunofluorescence staining (scale bar = 100 μm). **d** Statistical
893 analysis of neurons (Tuj^+ cells), astrocytes ($GFAP^+$ cells) and oligodendrocytes ($GalC^+$
894 cells) between the WFA- and DMSO-treated control groups (*$P \leq 0.05$). **e** Detection of

895 dopaminergic neurons derived from NSCs using immunofluorescence staining (Scale

896 bar = 100 μm). **f** Statistical analysis of the proportion of dopaminergic neurons (TH^+

897 Tuj^+ cells) in neurons (Tuj^+ cells) between the WFA and control groups (*$P \leq 0.05$). **g**

898 Assessment of the mRNA expression of genes regulating the pluripotency of stem cells

899 by quantitative RT-PCR (*$P \leq 0.05$).

900

901 **Table 1 Downregulated aggravator genes and the involved agonists**

Aggravator genes	Agonists (DrugBank)
ADRA2C	Brimonidine, Norepinephrine, Droxidopa, Clonidine, Bromocriptine, Apomorphine, Paliperidone, Ephedra sinica root, Metamfetamine, Xylometazoline, Agmatine, Oxymetazoline, Racepinephrine
DRD3	Ropinirole, Pramipexole, Apomorphine, Cariprazine, Pergolide, Bromocriptine, Lisuride, Cabergoline, Rotigotine, Dopamine, Levodopa, Captodiame, Dihydro-alpha-ergocryptine, Tianeptine
OPRD1	Codeine, Dextropropoxyphene, Hydrocodone, Morphine, Butorphanol, Fentanyl, Etorphine, 3-Methylthiofentanyl, Dimethylthiambutene, Loperamide, 3-Methylfentanyl, Oxycodone, Diamorphine, Tramadol, Methadone, Sufentanil, Carfentanil, Amitriptyline, Diphenoxylate, Levorphanol, Dihydromorphine, Remifentanil, Ketobemidone, Dextromethorphan, Opium, Loxicodegol, Butyrfentanyl, Metenkefalin, Hydromorphone

902

Supplementary Figure

Supplementary Fig. 1 Clinical aggravation of PD patients. a The overall aggravation of PD patients (N = 252). Although most patients are under drug treatment after enrollment, the disease condition is still in progression (Repeated measures ANOVA P = 9.15e-20). **b** The aggravation trajectory for each PD patient.

Supplementary Fig. 2 Heatmap of aggravator genes in independent PD patients (425 RNA-seq samples).

Supplementary Fig. 3 QQ plot of MWAS using baseline MDS-UPDRS total score as a clinical trait. As shown in the plot, almost all the CpGs on the diagonal of the plot and seldom the P-value of CpGs were smaller than expected, which indicates that little CpG was found to be significantly associated with this clinical trait.

Supplementary Fig. 4 Heatmap of cell types associated with PD aggravation. Abbreviations: Th1 cells, Type 1 T-helper cells; aDC, Activated dendritic cells; CD4+Tem, CD4+ effector memory T-cells; CD8+ Tcm, CD8+ central memory T cells; MSC, Mesenchymal stem cells; Th2 cells, Type 2 T-helper cells; HSC, Hematopoietic stem cells.

Supplementary Fig. 5 Identifying drugs and potential drug targets for PD. a

925 L1000CDS² analysis for drug discovery. DEGs in the pathway of regulating
926 pluripotency of stem cells (KEGG ID: hsa04550) were submitted to L1000CDS² to
927 predict potential agents. DEGs overlapping with background genes of withaferin A in
928 L1000 signatures were considered WFA-regulated genes. Five WFA-regulated genes
929 were confirmed by the validation datasets. **b** Downregulated aggravator genes and PD
930 drug targets in the neuron presynaptic terminal of dopaminergic synapse. The green
931 color indicates drug targets of PD, while the magenta color indicates aggravator gene.
932

933 **Supplementary Fig. 6 Morphology and immunofluorescent identification of NSCs.**
934 **a** Bright field image of suspended neurospheres at P1 (passage 1) that was cultured in
935 complete StemPro® NSC SFM for 6 days (Scale bar = 100 μm). **b** Bright field image
936 of adherent NSCs at P2 (passage 2) that were cultured in complete StemPro® NSC SFM
937 (scale bar = 100 μm). **c** Immunofluorescent identification of NSCs with primary mouse
938 anti-Nestin monoclonal antibody (ab6142, 1:100, Abcam, Cambridge, UK) (Scale bar
939 = 100 μm). **d** Merged fluorescence image of nestin and DAPI (scale bar = 100 μm).

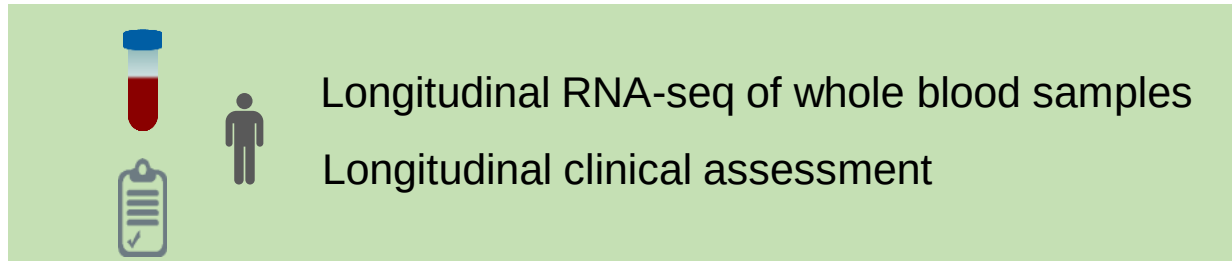
Longitudinal RNA-seq of whole blood samples
Longitudinal clinical assessment

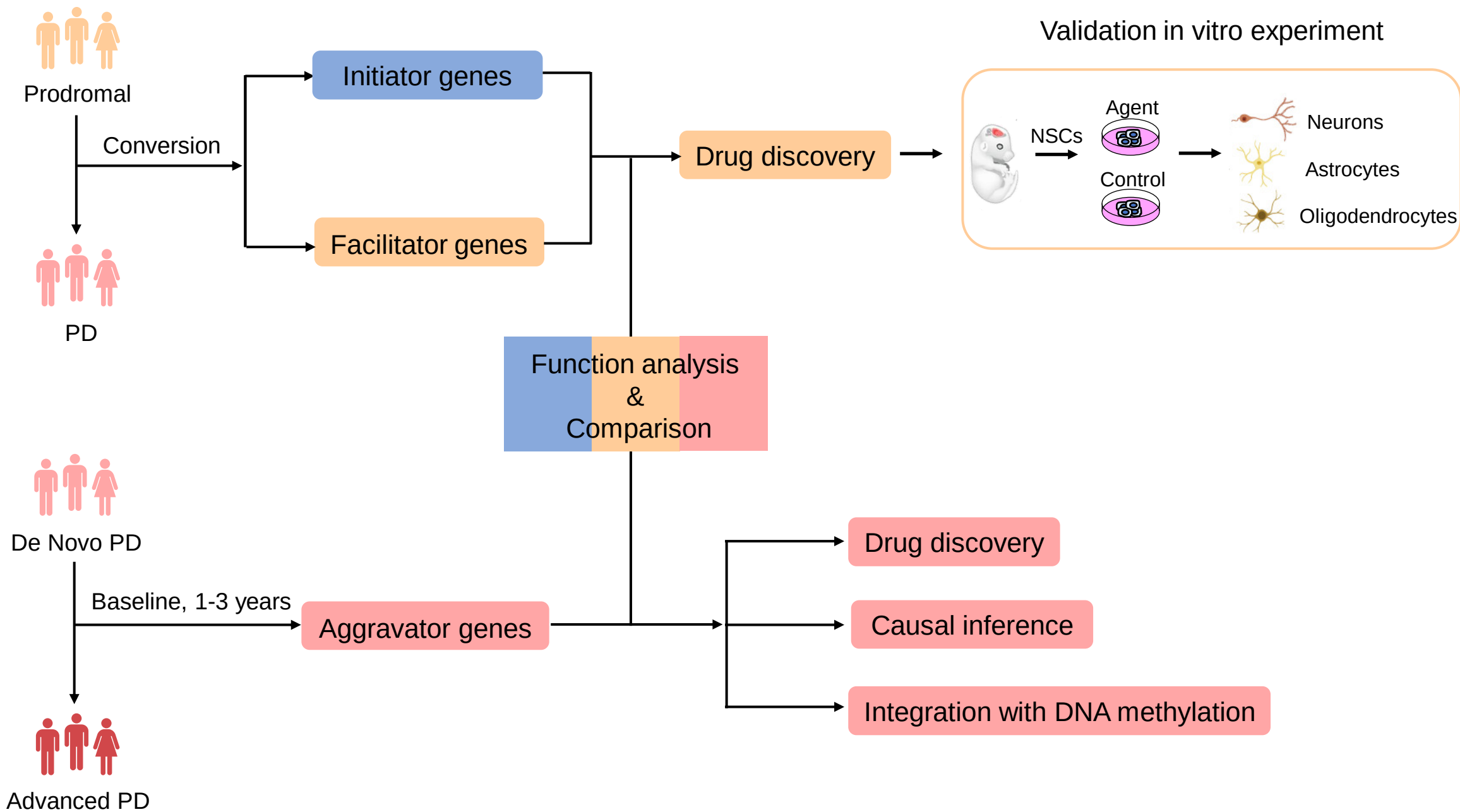
Prodromal
Conversion
PD
Initiator genes
Facilitator genes
Drug discovery
Validation in vitro experiment
NSCs
Agent
Control
Neurons
Astrocytes
Oligodendrocytes
Function analysis
&
Comparison
De Novo PD
Baseline, 1-3 years
Advanced PD
Aggravator genes
Drug discovery
Causal inference
Integration with DNA methylation

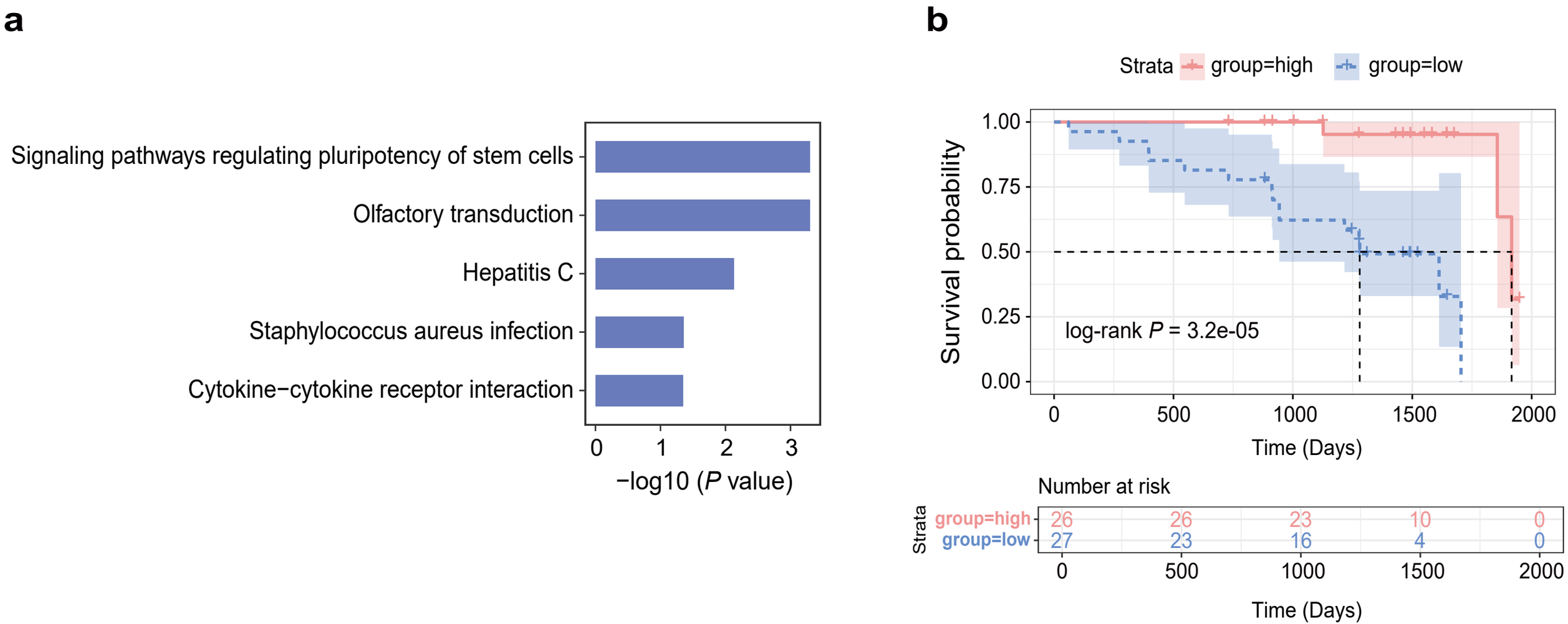
a
Signaling pathways regulating pluripotency of stem cells
Olfactory transduction
Hepatitis C
Staphylococcus aureus infection
Cytokine−cytokine receptor interaction
0
1
2
3
−log10 (P value)
b
Strata
group=high
group=low
Survival probability
1.00
0.75
0.50
0.25
0.00
log-rank P = 3.2e-05
0
500
1000
1500
2000
Time (Days)
Number at risk
Strata
group=high
26
26
23
10
0
group=low
27
23
16
4
0
0
500
1000
1500
2000
Time (Days)

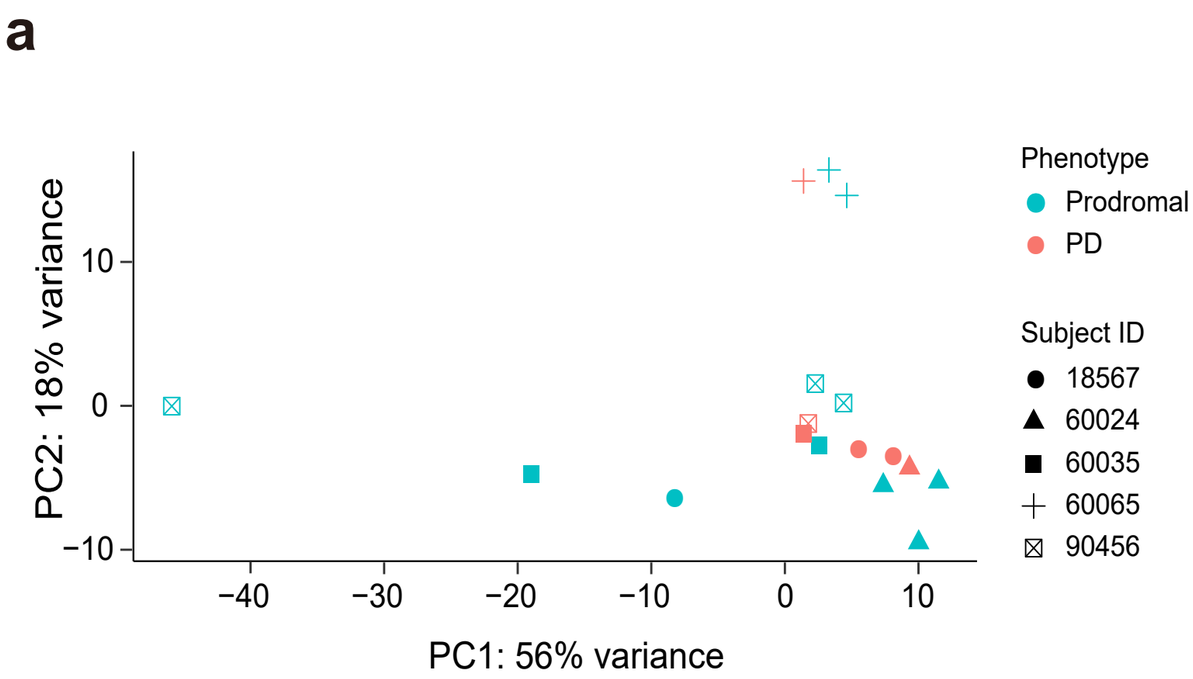
a
PC2: 18% variance
PC1: 56% variance
10
0
−10
−40
−30
−20
−10
0
10
Phenotype
Prodromal
PD
Subject ID
18567
60024
60035
60065
90456

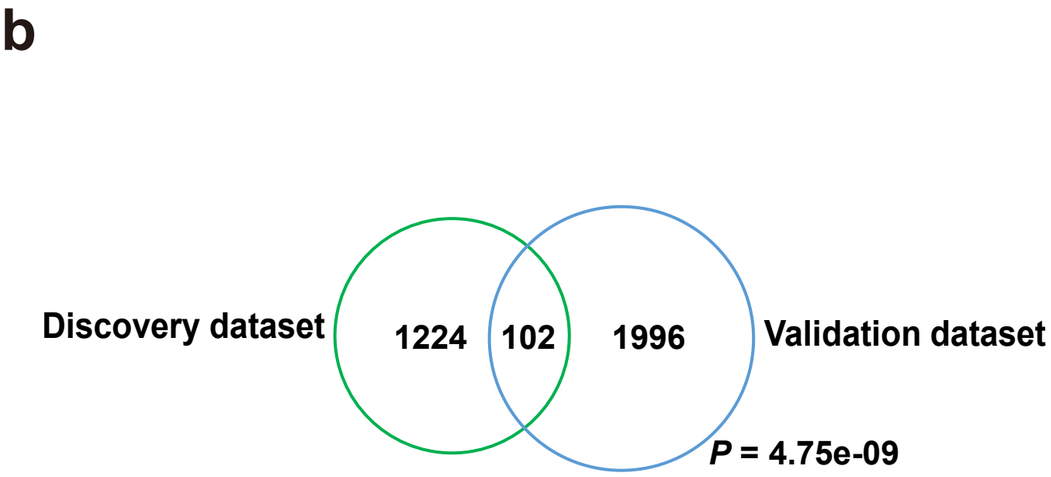
b
Discovery dataset
1224
102
1996
Validation dataset
P = 4.75e-09

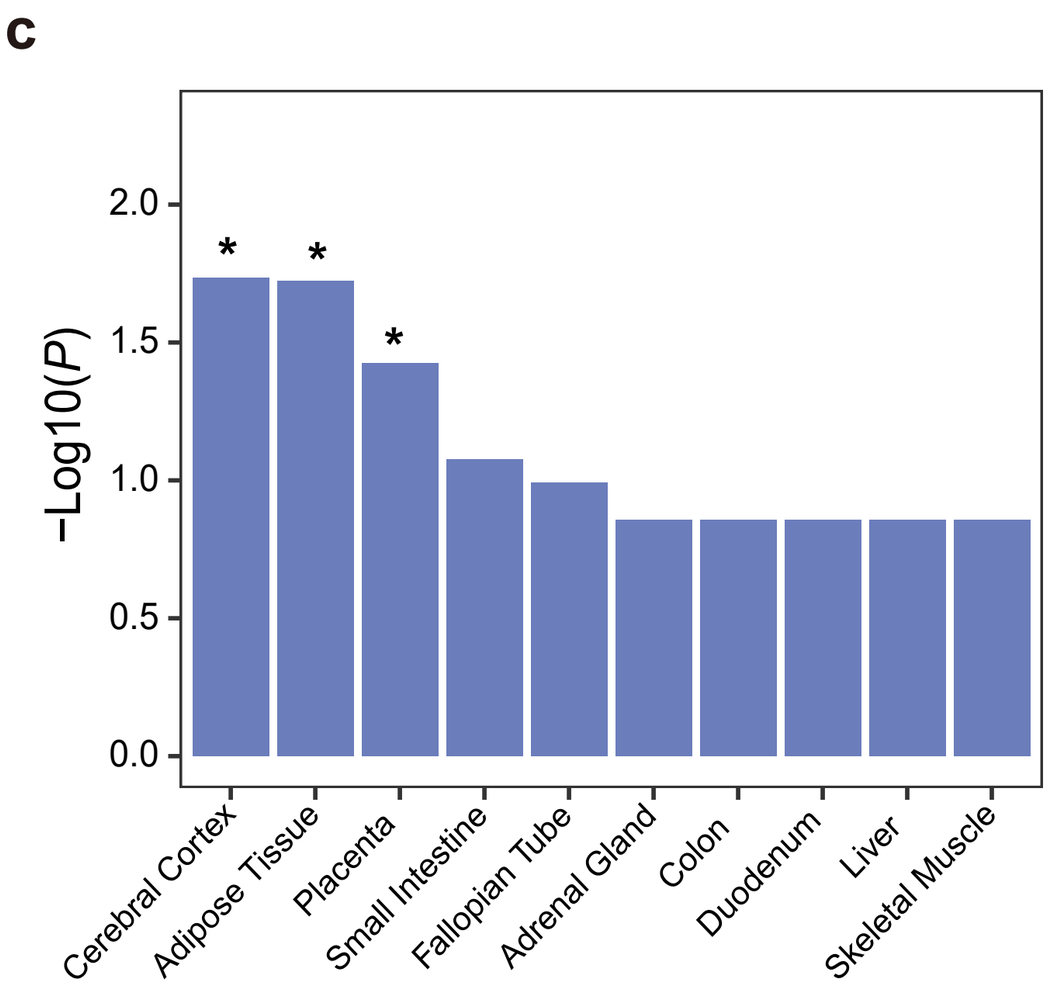
c
−Log10(P)
2.0
1.5
1.0
0.5
0.0
*
*
*
Cerebral Cortex
Adipose Tissue
Placenta
Small Intestine
Fallopian Tube
Adrenal Gland
Colon
Duodenum
Liver
Skeletal Muscle

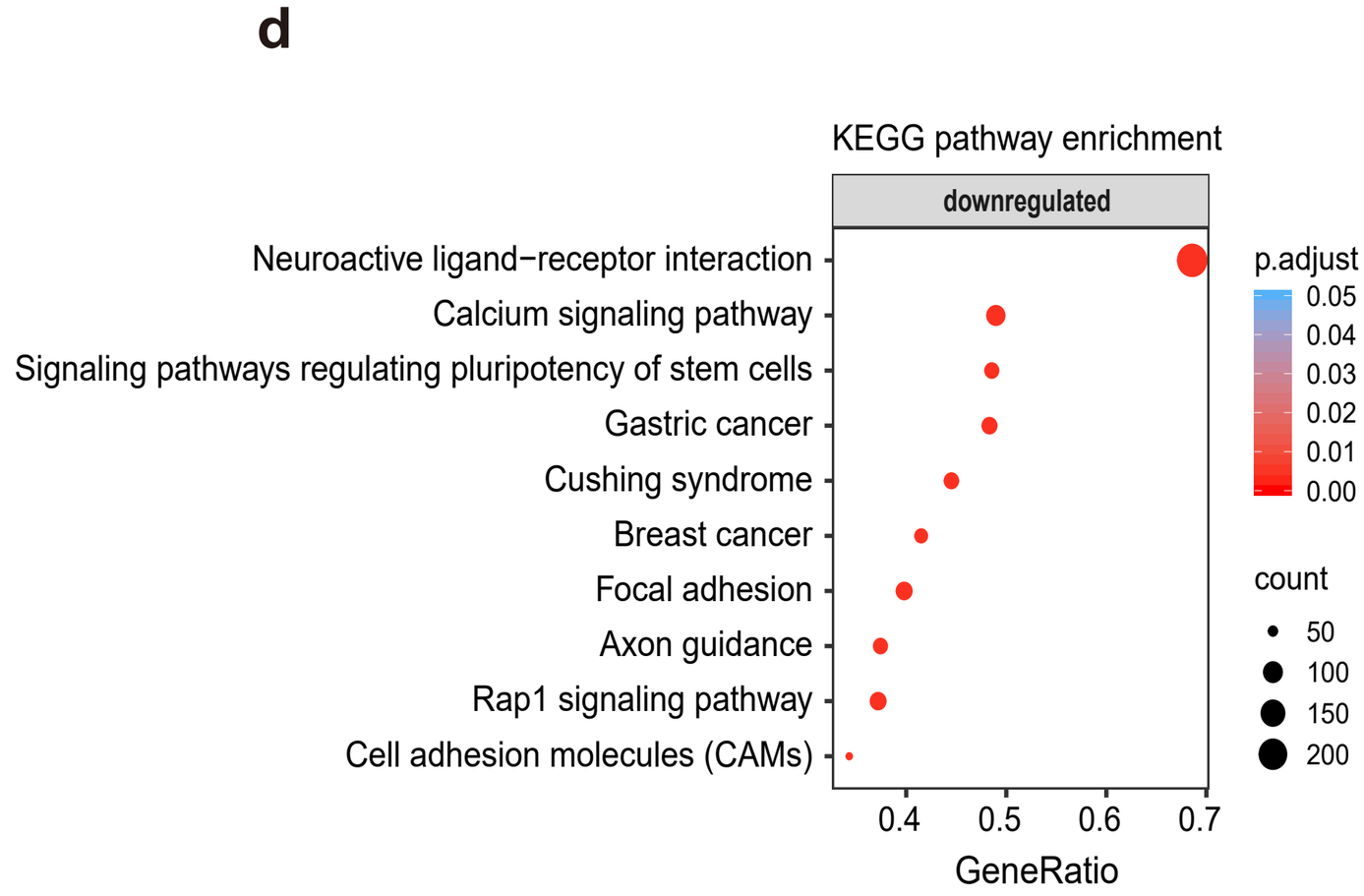
d
KEGG pathway enrichment
downregulated
Neuroactive ligand−receptor interaction
Calcium signaling pathway
Signaling pathways regulating pluripotency of stem cells
Gastric cancer
Cushing syndrome
Breast cancer
Focal adhesion
Axon guidance
Rap1 signaling pathway
Cell adhesion molecules (CAMs)
0.4
0.5
0.6
0.7
GeneRatio
p.adjust
0.05
0.04
0.03
0.02
0.01
0.00
count
50
100
150
200

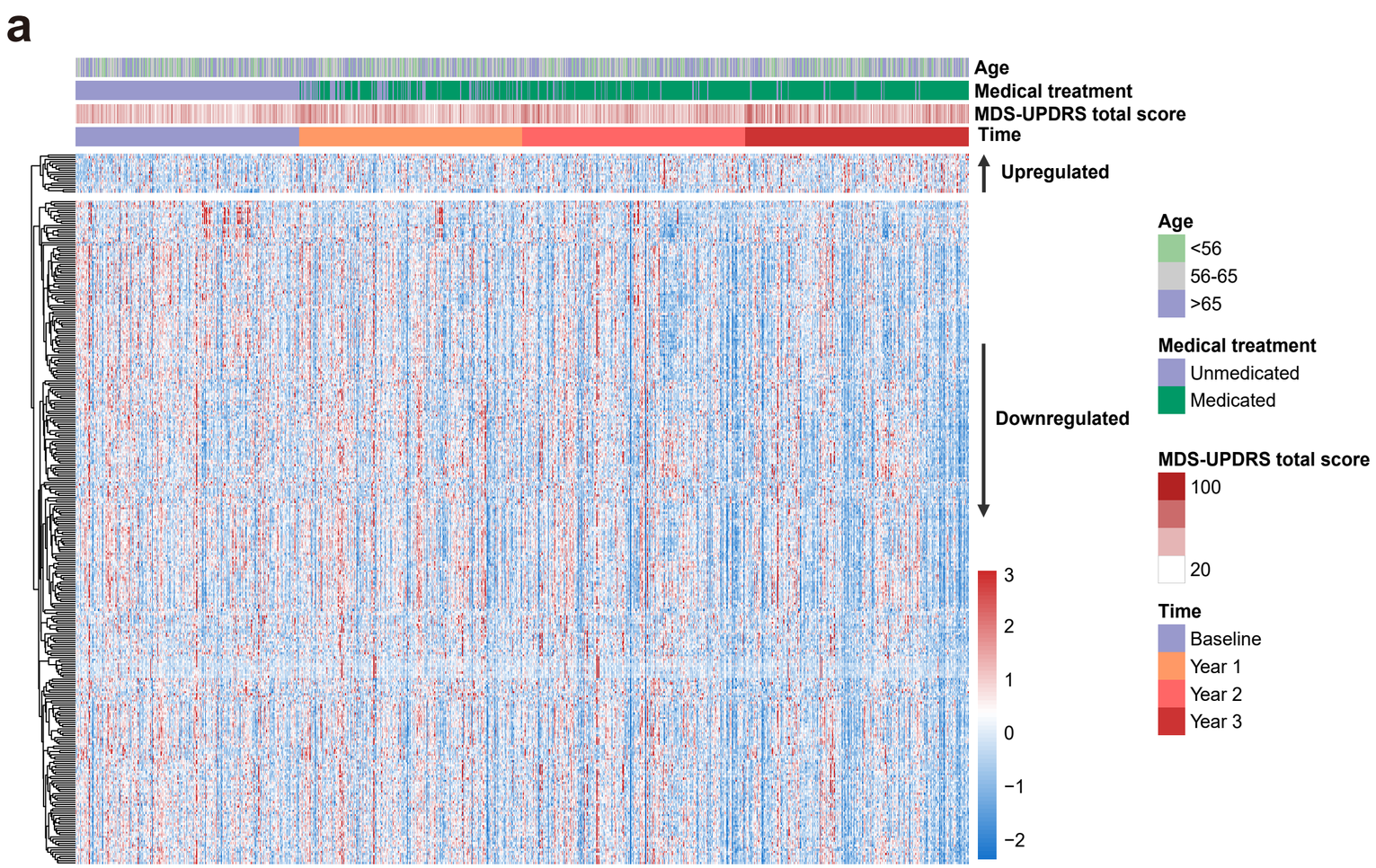
a
Age
Medical treatment
MDS-UPDRS total score
Time
Upregulated
Downregulated
3
2
1
0
−1
−2
Age
<56
56-65
>65
Medical treatment
Unmedicated
Medicated
MDS-UPDRS total score
100
20
Time
Baseline
Year 1
Year 2
Year 3

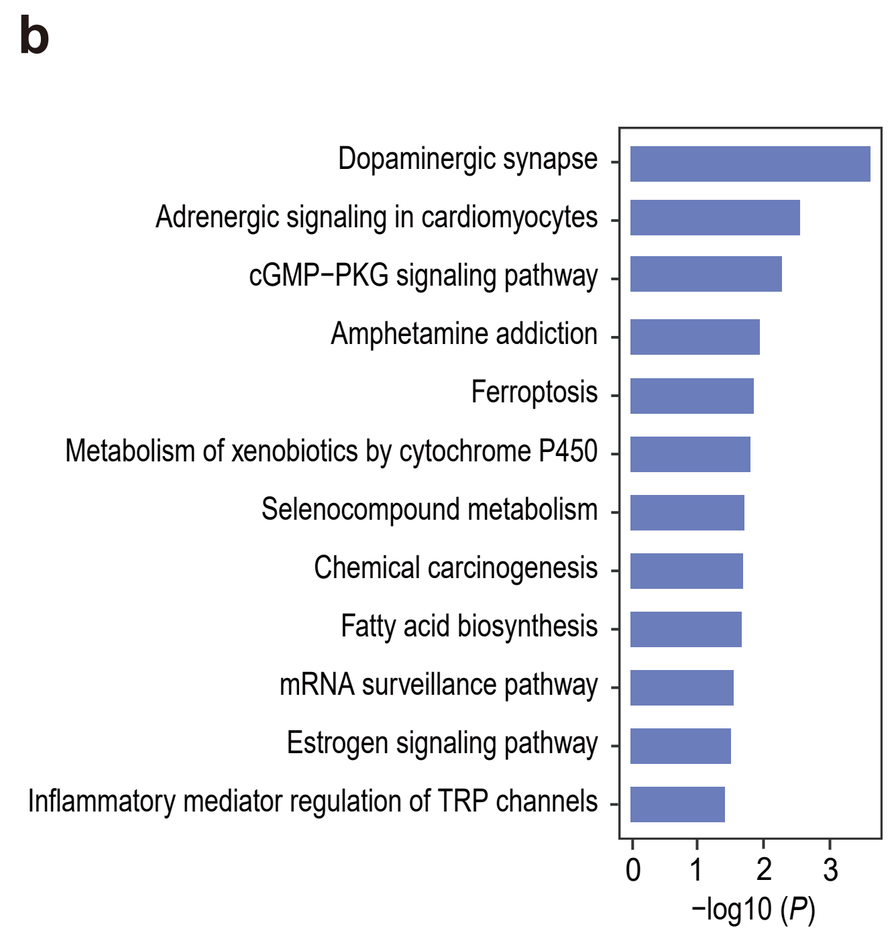
b
Dopaminergic synapse
Adrenergic signaling in cardiomyocytes
cGMP−PKG signaling pathway
Amphetamine addiction
Ferroptosis
Metabolism of xenobiotics by cytochrome P450
Selenocompound metabolism
Chemical carcinogenesis
Fatty acid biosynthesis
mRNA surveillance pathway
Estrogen signaling pathway
Inflammatory mediator regulation of TRP channels
0
1
2
3
−log10 (P)

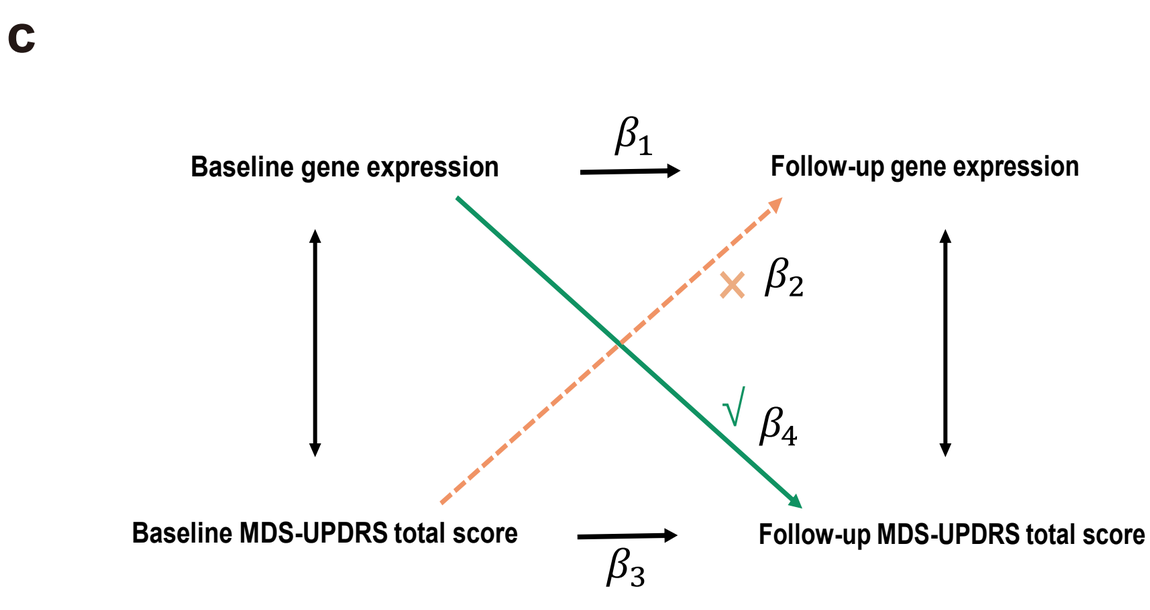
c
Baseline gene expression
Follow-up gene expression
Baseline MDS-UPDRS total score
Follow-up MDS-UPDRS total score
β_1
β_2
β_3
β_4

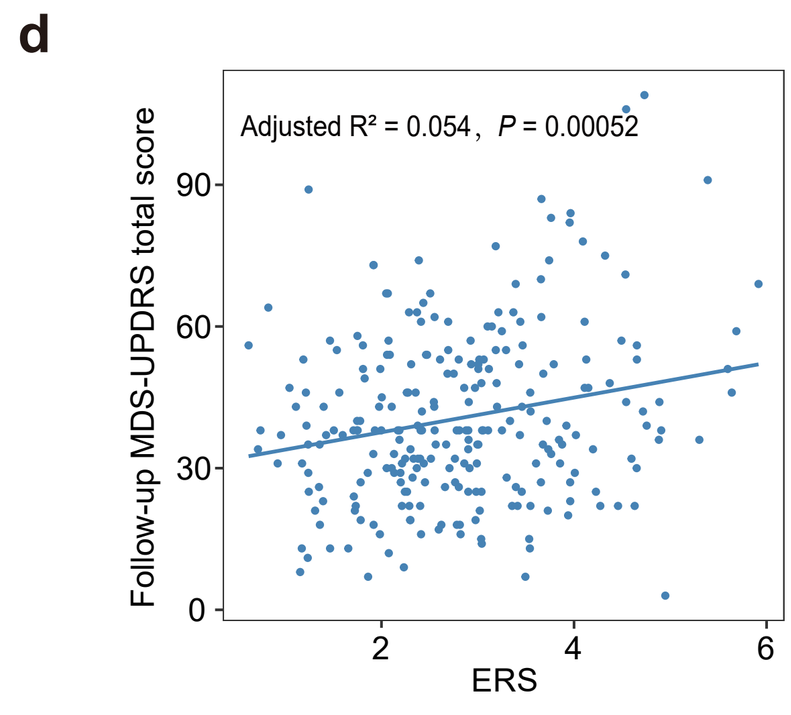
d
Adjusted R² = 0.054 , P = 0.00052
Follow-up MDS-UPDRS total score
0
30
60
90
2
4
6
ERS

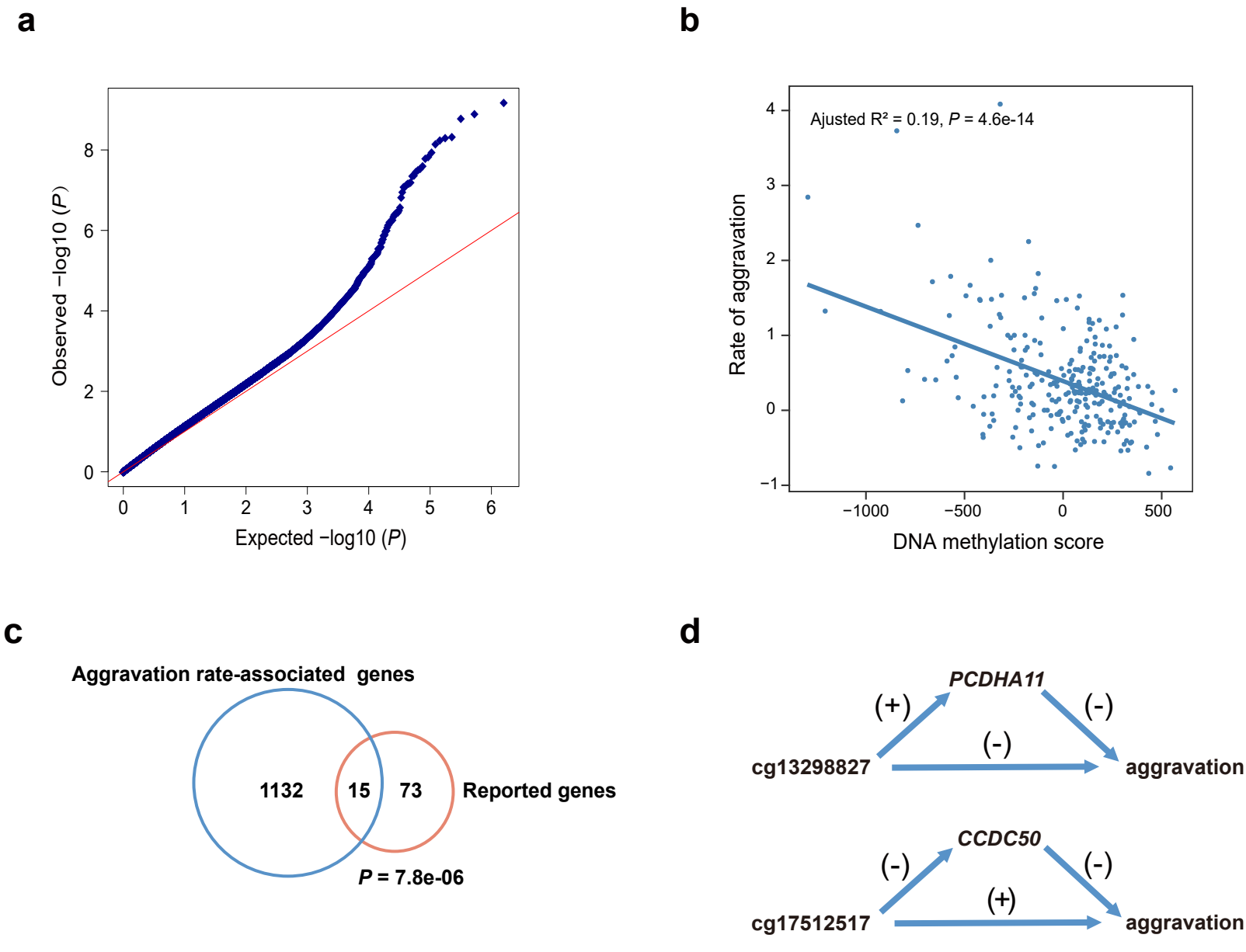
a
Observed −log10 (P)
Expected −log10 (P)
0
2
4
6
8
0
1
2
3
4
5
6
b
Ajusted R² = 0.19, P = 4.6e-14
Rate of aggravation
DNA methylation score
−1
0
1
2
3
4
−1000
−500
0
500
c
Aggravation rate-associated genes
1132
15
73
Reported genes
P = 7.8e-06
d
PCDHA11
(+)
(-)
(-)
cg13298827
aggravation
CCDC50
(-)
(-)
(+)
cg17512517
aggravation

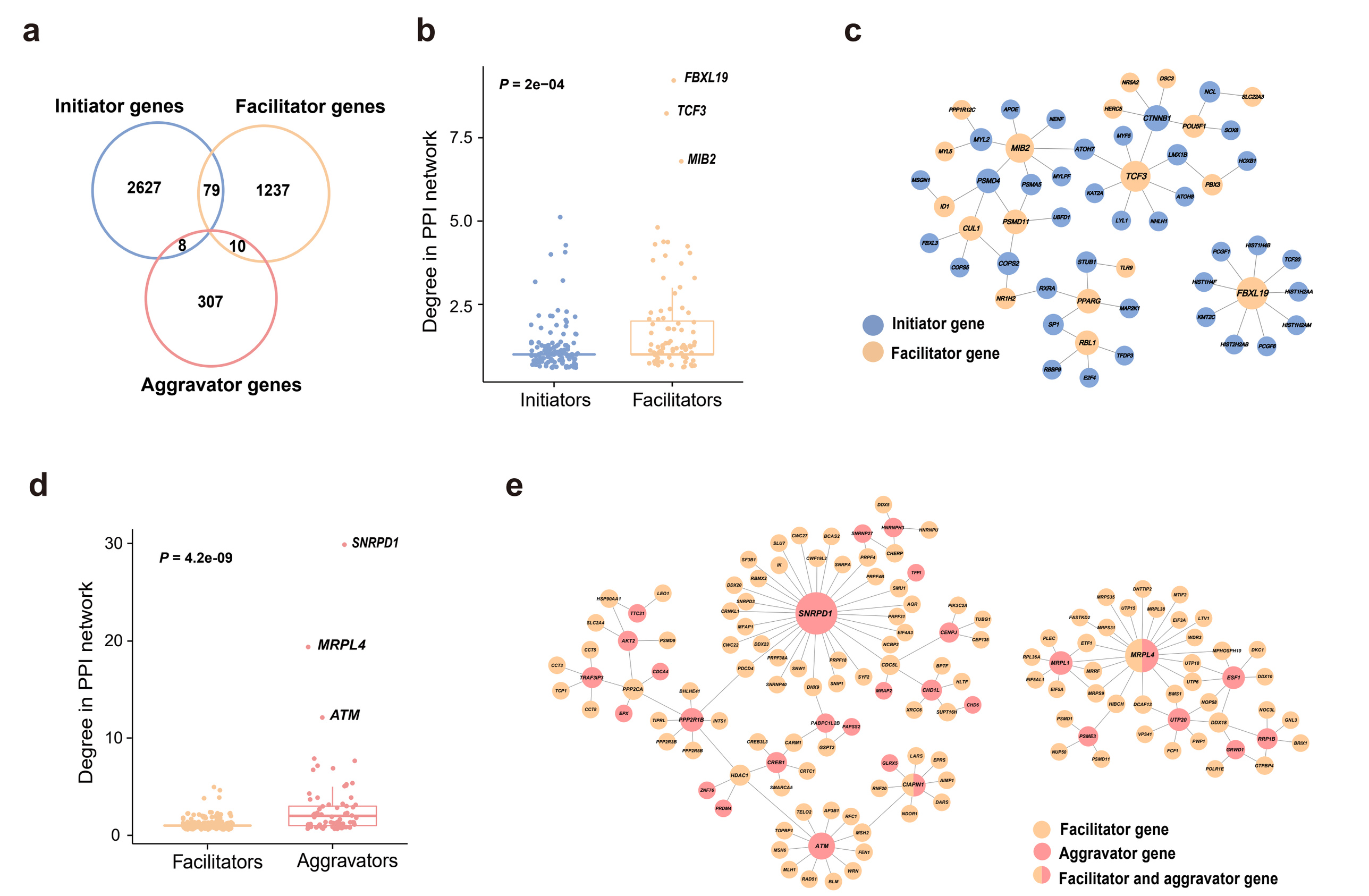
a
Initiator genes
Facilitator genes
Aggravator genes
2627
79
1237
8
10
307
b
P = 2e−04
FBXL19
TCF3
MIB2
Degree in PPI network
7.5
5.0
2.5
Initiators
Facilitators
c
Initiator gene
Facilitator gene
d
P = 4.2e-09
SNRPD1
MRPL4
ATM
Degree in PPI network
30
20
10
0
Facilitators
Aggravators
e
Facilitator gene
Aggravator gene
Facilitator and aggravator gene

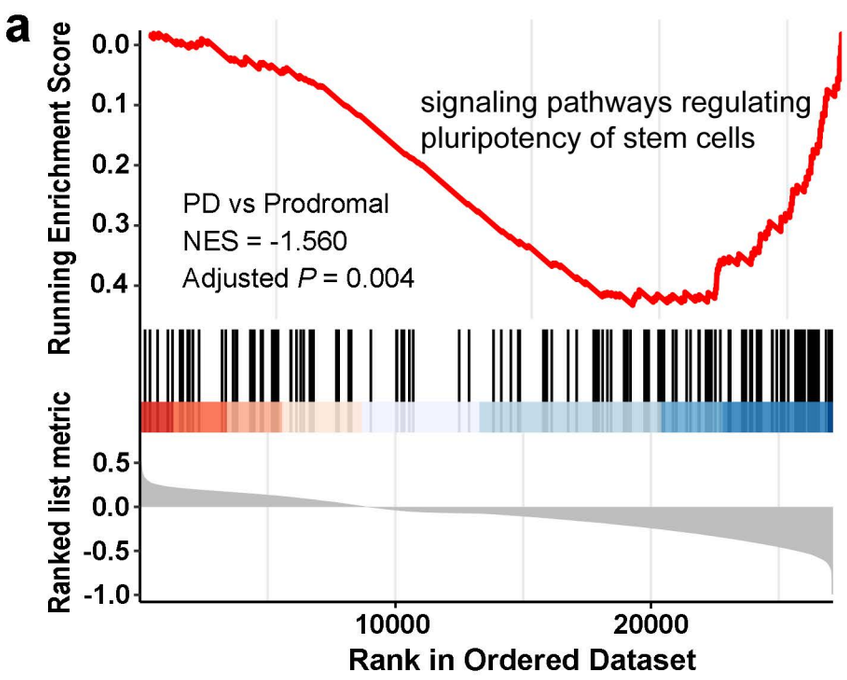
a
Running Enrichment Score
0.0
0.1
0.2
0.3
0.4
signaling pathways regulating
pluripotency of stem cells
PD vs Prodromal
NES = -1.560
Adjusted P = 0.004
Ranked list metric
0.5
0.0
-0.5
-1.0
10000
20000
Rank in Ordered Dataset

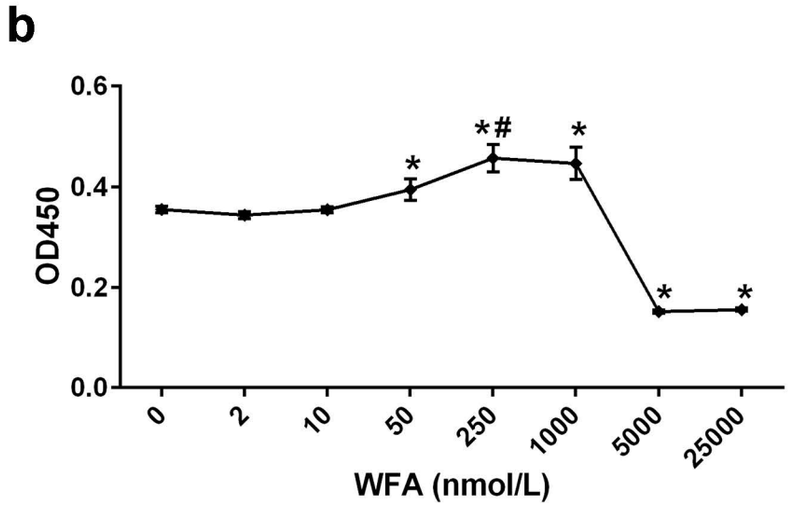
b
OD450
0.6
0.4
0.2
0.0
*
*#
*
*
*
0
2
10
50
250
1000
5000
25000
WFA (nmol/L)

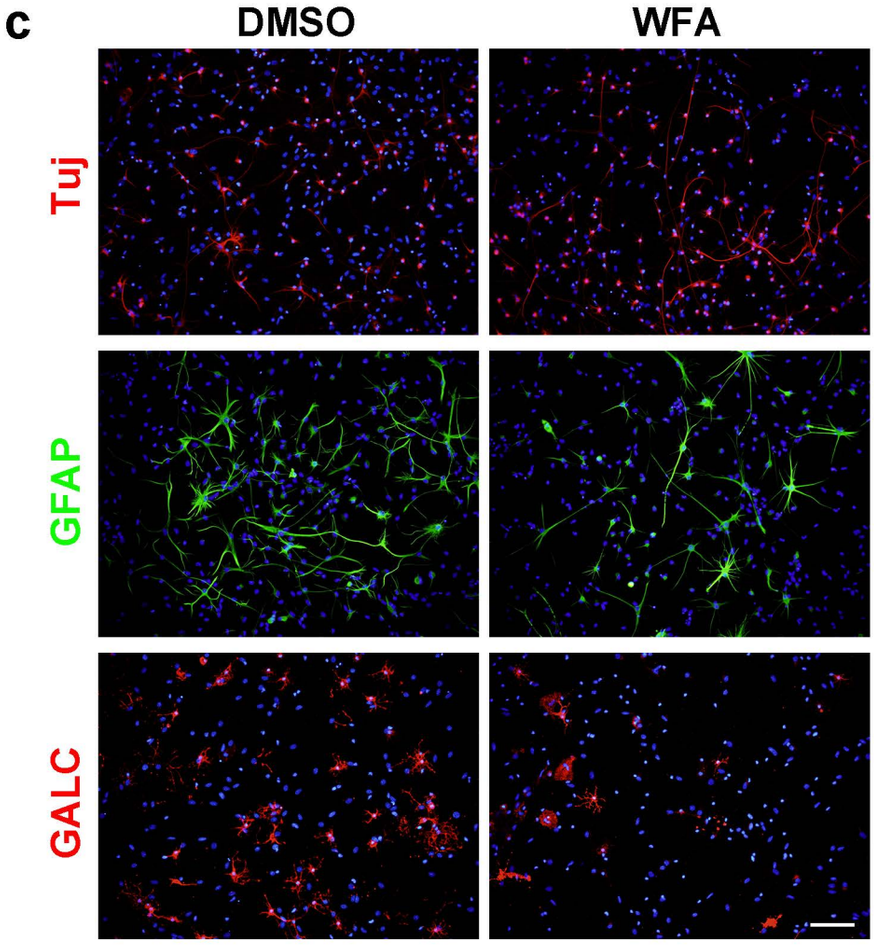
c
DMSO
WFA
Tuj
GFAP
GALC

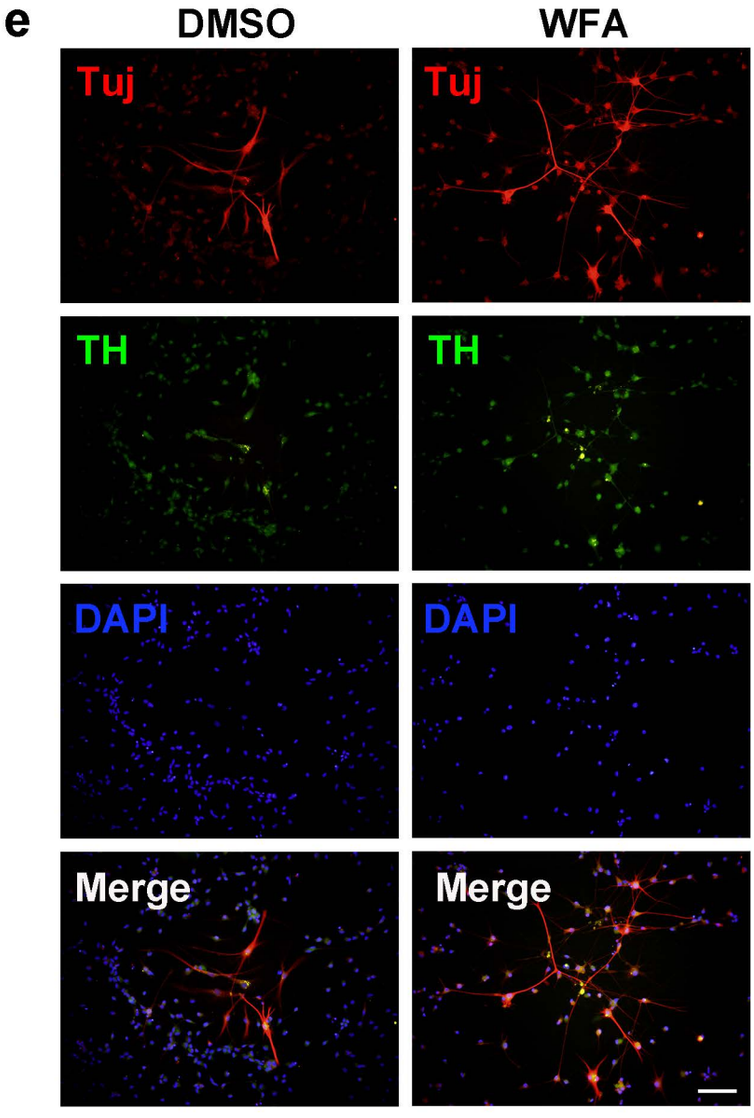
e
DMSO
WFA
Tuj
Tuj
TH
TH
DAPI
DAPI
Merge
Merge

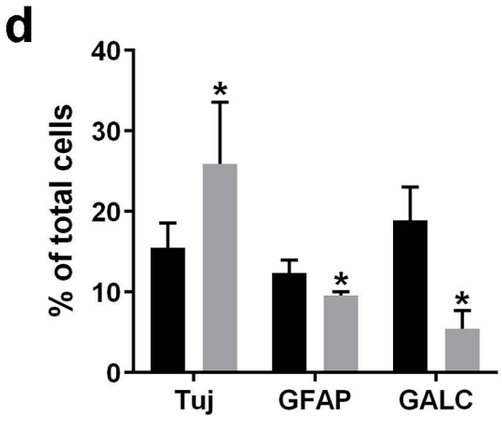
d
% of total cells
40
30
20
10
0
*
*
*
Tuj
GFAP
GALC

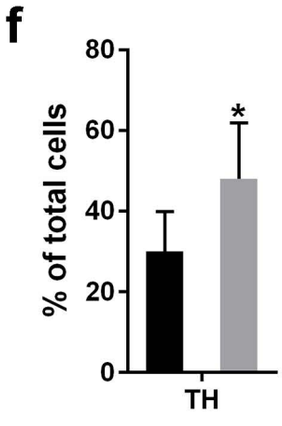
f
% of total cells
80
60
40
20
0
*
TH

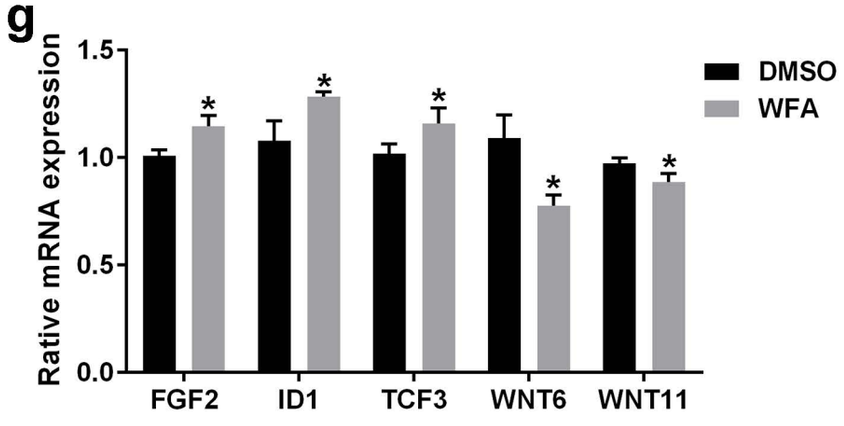
g
Rative mRNA expression
1.5
1.0
0.5
0.0
DMSO
WFA
*
*
*
*
*
FGF2
ID1
TCF3
WNT6
WNT11